UNIVERSITY OF CALIFORNIA, SAN DIEGO

DNA Binding Specificity of the p73 DNA-Binding Domain

A Thesis submitted in partial satisfaction of the requirements for the degree
Master of Science

in

Chemistry

by

Pui Wah Tse

Committee in charge:

Professor Hector Viadiu, Chair
Professor Daniel Donoghue
Professor Ulrich Muller

2011

The Thesis of Pui Wah Tse is approved and it is acceptable in quality and form for publication on microfilm and electronically:

Chair

University of California, San Diego

2011

TABLE OF CONTENTS

LIST OF ABBREVIATIONS AND SYMBOLS

AUC	analytical ultracentrifugation
bp	base pair
c(s)	continuous size distribution
K_d	dissociation constant
DTT	Dithiothreitol
DBD	DNA-binding domain
E. coli	*Escherichia coli*
ID	inhibitory domain
IPTG	isopropyl-β-D-thiogalactopyranoside
kDa	kilodalton
NGF	nerve growth factor
OD	optical density
PMSF	phenylmethanesulfonylfluoride
Pu	purine
Py	Pyrimidine
REs	response elements
S-value	sedimentation coefficient
SDS-PAGE	sodium dodecyl sulfate polyacrylamide gel electrophoresis
SAM	Sterile Alpha Motif
TD	tetramerization domain
TAD	transactivation domain

LIST OF FIGURES

LIST OF TABLES

ACKNOWLEDGEMENTS

First and foremost, I would like to sincerely thank my advisor Dr. Hector Viadiu, for giving me an opportunity to study in his lab. His guidance, support, and encouragement have been helped and motivated me throughout my graduate studies. I greatly appreciate the time that he has spent on my project. Without his guidance and help, this thesis would not have been possible.

I would like to thank Dr. Abdul S. Ethayathulla, for teaching me all the lab techniques when I first joined the lab. Thanks for being patient with me all the time and giving me all the advices and help on my project. I would like to thank my friend Nikki Cheung, for guiding me to become an independent researcher and giving me suggestions and help. Thanks for her caring and tremendous encouragement throughout these years. I would also like to thank the rest of the past and present lab members, especially Dr. Hiroyuki Akama, Michelle Chan, Ana Ramos, and Kate Kim, for being supportive and helpful, and sharing all the fun with me in the lab.

I gratefully thank my friend Dr. Vivien Wang, for her enormous supports, suggestions, and help. Thanks for taking care of me when I was stressed and depressed. I would also like to thank my friends, Connie Yu, Long Truong, Julianna Wang, and Nicole Lam, for being supportive all these years. In addition, I offer my regards and blessings to all of those who supported me in any aspect during the completion of this project.

Lastly, I would like to thank my parents and my sister for their love and care. Thanks for giving me support and encouragement all the time.

ABSTRACT OF THE THESIS

DNA Binding Specificity of the p73 DNA-Binding Domain

by

Pui Wah Tse

Master of Science in Chemistry

University of California, San Diego, 2011

Professor Hector Viadiu, Chair

p73 is a sequence-specific transcription factor that belongs to the p53 family. It plays an important role in cell development and regulation, and initiating cell cycle arrest and apoptosis under cellular stresses. In p53 family proteins, p53 is considered as “the guardian of genome” with a primary role of tumor suppressor. However, mutations in p53, particularly in DNA-binding domain (DBD), are found in 50% of human cancers while p73 is rarely mutated.

Therefore, it has been suggested that p73 can replace the functions of p53 mutants. The overall domain architecture of p53 family is similar with highly conserved DBD among the family members. The goal of this thesis is to study the DNA binding properties of p73 DBD using analytical ultracentrifugation and fluorescence anisotropy. Chapter 1 introduces transcription regulation, the p53 protein family and its pathway, and p73 isoforms. Chapter 2 studies the minimum length of DNA required for p73 DNA binding which has showed that p73DBD binds to a minimum 6 bp half-site as a dimer. Chapter 3 studies the p73 DNA binding specificity at each nucleotide position within the consensus half-site. In agreement with the previous crystal structures, the results have indicated that the cytosine and the guanine at position 4 are the most critical nucleotides in the consensus sequence. In addition, the p73 DNA binding affinity is salt concentration dependent. Chapter 4 described the expression and purification of p73 isoforms in order to further study p73 DNA binding property in the full-length content in the future.

Chapter 1

Introduction

A. Transcription regulation

In eukaryotes, gene expression is regulated by various steps, and it is believed that transcription initiation is the key step in it. The transcription of protein encoding genes is typically called *cis*-acting transcriptional regulatory DNA element. It contains recognition sites for *trans*-acting DNA binding transcription factors, which either enhance or repress transcription (Maston et al., 2006). The protein-coding genes recognized by RNA polymerase II can be classified into three groups: general transcription factors (GTFs), promoter-specific activators (PSAs), and co-activators (Conaway et al., 2005; Malik and Roeder, 2005).

The GTFs initiate transcription by assembling on the core promoter region and forming transcription preinitiation complex, which directs RNA polymerase II to transcription start site.

The PSAs are termed as activators. In general, they are sequence-specific DNA-binding proteins whose recognition sites are usually present in sequences upstream of the core promoter (Ptashne and Gann, 1997). They are classified based on their DNA-binding domains (DBDs) binding to specific class of DNA sequences. In addition to a sequence-specific DBD, a typical activator also contains a separate transactivation domain (TD), which is required for the activator to stimulate transcription (Figure 1.1). The DNA binding sites for these activators are generally 6-12 bp, and their binding specificities are dictated by 4-6 bp within the sites. In general, the activators form heterodimers and/or homodimers, tetramers, thus their binding sites are generally composed of two

half-sites. Although an activator can bind to wide variety of sequence variants that conform to the consensus, the precise sequence can affect the binding strength of activator, which may be biologically important in situations such as early development, in which activators are distributed in a concentration gradient. Finally, the particular sequence of a transcription factor-binding site can affect the structure of a bound activator which alters its activity. Various studies have shown that the relative orientation of the half-sites, as well as the spacing between them, play a major role in directing the regulatory action of activators (Fourel et al., 2004; Lefstin and Yamamoto, 1998; Remenyi et al., 2004; Scully et al., 2000). p53 family proteins, p53, p63, and p73, are transcription factors which can act as activator and repressor when they bind to certain p53 promoter sequences. Therefore, one of the main objectives of this thesis is to understand the effect of the sequence variation in the p53 consensus half-site response element.

B. The p53 protein family

p53 family proteins are sequence-specific transcriptional factors that are involved in initiating cell cycle arrest and apoptosis in response to cellular stresses and DNA damage. The p53 protein family consists of three members, p53, p63, and p73. p53 was the first protein discovered in 1979 that associates with the oncogenic T antigen from SV40 virus (Lane and Crawford, 1979; Linzer and Levine, 1979). Further studies have shown that p53 acts as a tumor suppressor that plays a crucial role in human cancers (el-Deiry et al., 1992; Shaw

et al., 1992; Yonish-Rouach et al., 1991). Twenty years later, two p53 homologous genes, *TP73* and *TP63*, which play an important role in cell development and regulation were identified. In 1997, the human *TP73* gene was discovered in a region of chromosome 1p36, which is frequently deleted in neuroblastoma (Kaghad et al., 1997). In 1998, the human *TP63* gene was discovered in chromosome 3q27, and it was found widely expressed in the basal cells of epithelial tissues (Yang et al., 1998). Later, it was also discovered that p73 and p63 have the ability to induce cell cycle arrest and apoptosis during cellular stress (Gressner et al., 2005; Irwin et al., 2000). Although p73 and p63 genes are homologues of the p53 gene, the p73 and p63 knockout mice show developmental abnormalities instead of increased tumorigenesis (Yang et al., 1999; Yang et al., 2000).

C. The p53 protein family pathway

The p53 family proteins are transcription factors that activate the transcription of their target genes in response to DNA damage or cellular stresses. In the resting cells, p53 family proteins are regulated by negative regulators. MDM2 binds to p53 to mediate its ubiquitination and proteasomal degradation (Kubbutat et al., 1997). p63 and p73 are regulated by its own numerous N-terminal truncated isoforms (Grob et al., 2001; Serber et al., 2002). Upon DNA damage and other cellular stresses, specific kinases are activated, which modify the N-terminal transactivation domain (TAD) of p53 family proteins through post-translational modifications (PTMs), such as phosphorylation,

methylation, and acetylation. For example, p53 is phosphorylated by Chk1 or ATM, and p73 is phosphorylated by Chk1 or c-Abl. The PTMs of TAD prevent the binding of negative regulators and increase the level of p53 family proteins. The PTM modified proteins are imported into nucleus where they bind to specific promoter region and recruit transcriptional co-activators. For example, the phosphorylated p53 family proteins induce recruitment of the transcriptional co-activator p300/CBP to mediate the acetylation of target genes. Examples of other known target genes are *p21*, *Bax* and *PUMA* which will induce cell cycle arrest, DNA repair, or apoptosis (Figure 1.2) (Pietsch et al., 2008).

D. Domain organization of p53 family proteins

The proteins of the p53 family share similar domain architecture with three major domains: a N-terminal transactivation domain (TAD), a central DNA-binding domain (DBD), and a tetramerization domain (TD). p63 and p73 also contain extended C-terminal domain with a sterile alpha motif domain (SAM) and an inhibitory domain (ID), which is absent in p53 (Figure 1.3).

Transactivation Domain (TAD)

The TAD is located at the N-terminus of every member of p53 protein family, and it regulates the transcriptional activities of the p53 family proteins. p73 shares 25% similarity to p53 and 40% to p63. The TAD of the p53 family proteins recruits the transcriptional co-activator p300/CBP and mediates the transcription function (Avantaggiati et al., 1997). However, the TAD also interacts with the

negative regulators. For example, p53 is negatively regulated by MDM2, which leads to its ubiquitination and proteasomal degradation (Haupt et al., 1997; Kubbutat et al., 1997). MDM2 also binds to the TAD of p63 and p73, but it does not promote proteasomal degradation; instead, MDM2 blocks the interaction of p63 and p73 with the transcriptional co-activator and further represses their transcriptional activities (Zeng et al., 1999).

DNA-Binding Domain (DBD)

The DBD is the most conserved domain in the p53 family proteins. The DBD of p73 has 58% similarity to p53 and 85% to p63. It is a sequence-specific DNA binding domain that recognizes and binds to the specific DNA response elements (REs) to activate the transcriptional function. The canonical p53 RE consists of two 10 bp half-sites with a consensus sequence of Pu-Pu-Pu-C-A/T-T/A-G-Py-Py-Py (Pu=purine, and Py=pyrimidine) separated by 0-13 bp (el-Deiry et al., 1992; Lokshin et al., 2007; Smeenk et al., 2008). A monomer of DBD binds to a 5 bp quarter-site, and a tetramer binds to a 20 bp full-site RE to activate the transcription of target genes to induce cell cycle arrest and apoptosis (Chen et al., 2010; Cho et al., 1994; Ho et al., 2006; Kitayner et al., 2006; Kitayner et al., 2010; Malecka et al., 2009; Petty et al., 2011).

Tetramerization Domain (TD)

The TD of p73 has 35% similarity to p53 and 60% to p63. The active form of the p53 family proteins is a tetramer, and the TD promotes the formation of

tetramer (Chene, 2001). Since the TD of the p53 family proteins is conserved, it is suggested that p53 family proteins can form homotetramers as well as heterotetramers. Recently, *in vitro* studies revealed that the TDs of p63 and p73 interact with each other and form heterotetramers, and the heterotetramer consisting of two homodimers is the most stable p63/p73 form (Coutandin et al., 2009).

The C-terminal Domains

The C-terminal domain of p53 is a small 30 amino acids long regulatory domain rich in lysines and arginines (Viadiu, 2008). It was found to regulate the activities of p53 by post-translational modification such as phosphorylation, acetylation, methylation, and ubiquitination (Kim and Deppert, 2006; Liu and Kulesz-Martin, 2006).

p73 and p63 contain a drastically different C-terminus with two domains, SAM and ID, which are absent in p53. p73 C-terminus shares 50% similarity with p63. The SAM domain is a globular domain consists of ~70 amino acids, which is important in the cell development and regulation that involves in interactions with other proteins and RNA (Schultz et al., 1997). The ID regulates the transcriptional activities of p73 and p63 by interacting with the TAD or preventing the association with transcription coactivators (Liu and Chen, 2005; Serber et al., 2002).

E. The p73 gene and its isoforms

Human p73 gene (*TP73*) is located at chromosome 1p36 and exists as different isoforms generated by two promoters and alternative splicing. It consists of 14 exons as shown in Figure 1.4a, which encodes different p73 isoforms. Two different promoters in *TP73* gene generate two major isoforms, TAp73 with transactivation domain and the N-terminal truncated p73 (ΔNp73) which lacks TAD (Figure 1.4b) (Ishimoto et al., 2002; Pozniak et al., 2000; Yang et al., 2000). TAp73, which has TAD, is transcriptionally active and ΔNp73, which lacks of TAD, is transcription inactive. ΔNp73 is a dominant-negative inhibitor or negative regulator of transcription activity, by interacting with TAp73 and also competes for sequence specific DNA binding in the promoter region (Grob et al., 2001; Stiewe et al., 2002). Since TAp73 and ΔNp73 have opposite effects in cells, the balance between TAp73 and ΔNp73 determine the biological function of the p73 gene. Apart from these two major isoforms, alternative splicing of p73 gene in exon 10-13 generates seven other major isoforms (α, β, γ, δ, ε, ζ, and η) that have different transcriptional activities (De Laurenzi et al., 1998; De Laurenzi et al., 1999; Kaghad et al., 1997).

ΔNp73 plays a major role in developing neuronal cells. During neuronal development, the availability of the nerve growth factor (NGF) increases, which maintains the level of ΔNp73 high enough to bind to the promoter region of TAp73 and inhibit the apoptotic function of p73, resulting in the survival of the neuronal cells. Decrease in NGF leads to decreased cellular level of ΔNp73 and increase in TAp73 binding to the promoter region, which induces apoptosis of the

neuronal cells (Pozniak et al., 2000; Yang et al., 2000). Since ΔNp73 is important in neuronal development, the neuronal defects seen in the p73 knockout mice are due to the absence of the ΔNp73 (Pozniak et al., 2000). In order to further understand the role of p73 in tumorigenesis, TAp73 selectively deficient mice were used. The results showed that tumors increase in the absence of TAp73, demonstrating the tumor suppressor function of p73 (Tomasini et al., 2008).

F. Focus of Study

p53 has been described as “the guardian of the genome” to refer its important role as tumor suppressor. However, p53 is the most frequently mutated protein in cancer and 50% of human tumors are caused by mutated p53. More than 90% of p53 mutations are located in the DBD, and they are often missense mutations (Hollstein et al., 1994; Hollstein et al., 1991). p53 mutants lose the transactivation function and inhibit wild-type p53 by forming heterotetramers. In contrast, p73 is rarely mutated in cancerous cells (Melino et al., 2002). It also binds to the p53 REs to activate the transcription of p53 target genes. Therefore, it has been suggested that p73 can replace the function of mutant p53 (Bell and Ryan, 2007; Melino et al., 2003). It is crucial to study the DNA binding properties of p73DBD in order to understand the mechanism of how it binds to the specific DNA sequence. The goal of this thesis is to study the DNA binding properties of p73 DBD using analytical ultracentrifugation (AUC) and fluorescence anisotropy. I am focusing on determination of DNA specificity requirements for p73 DBD to bind to half-site RE. I aim to understand the contribution of each nucleotide within

the consensus half-site to p73 binding. Recombinant human p73 DNA binding domain (DBD) from residue 115 to 312 was used for all the experimental analysis. I also started experiments to extend my work with longer p73 isoforms to further study the contributions of other p73 domains to DNA binding.

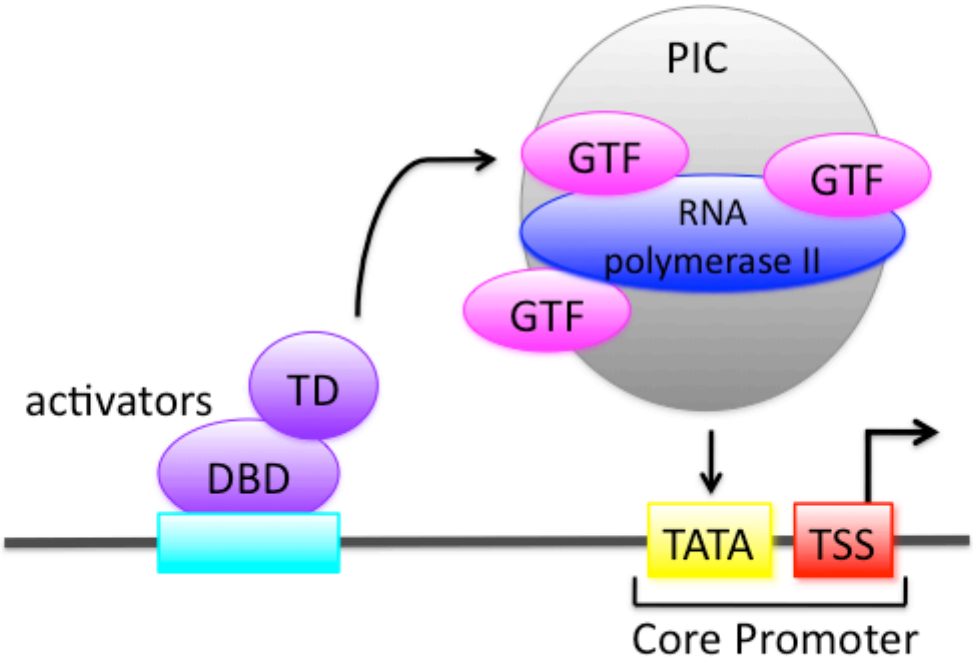

Figure 1.1. The eukaryotic transcription. The eukaryotic transcription is classified into: (i) The classical general transcription factors (GTFs) initiate transcription by assembling on the core promoter region and forming transcription preinitiation complex (PIC), which directs RNA polymerase II to transcription start site (TSS). (ii) Promoter dependent transcription factors: The transcriptional activity is stimulated by activators. The activators consist of DNA-binding domain (DBD) and transactivation domain (TD), which are required to stimulate the formation of PIC.

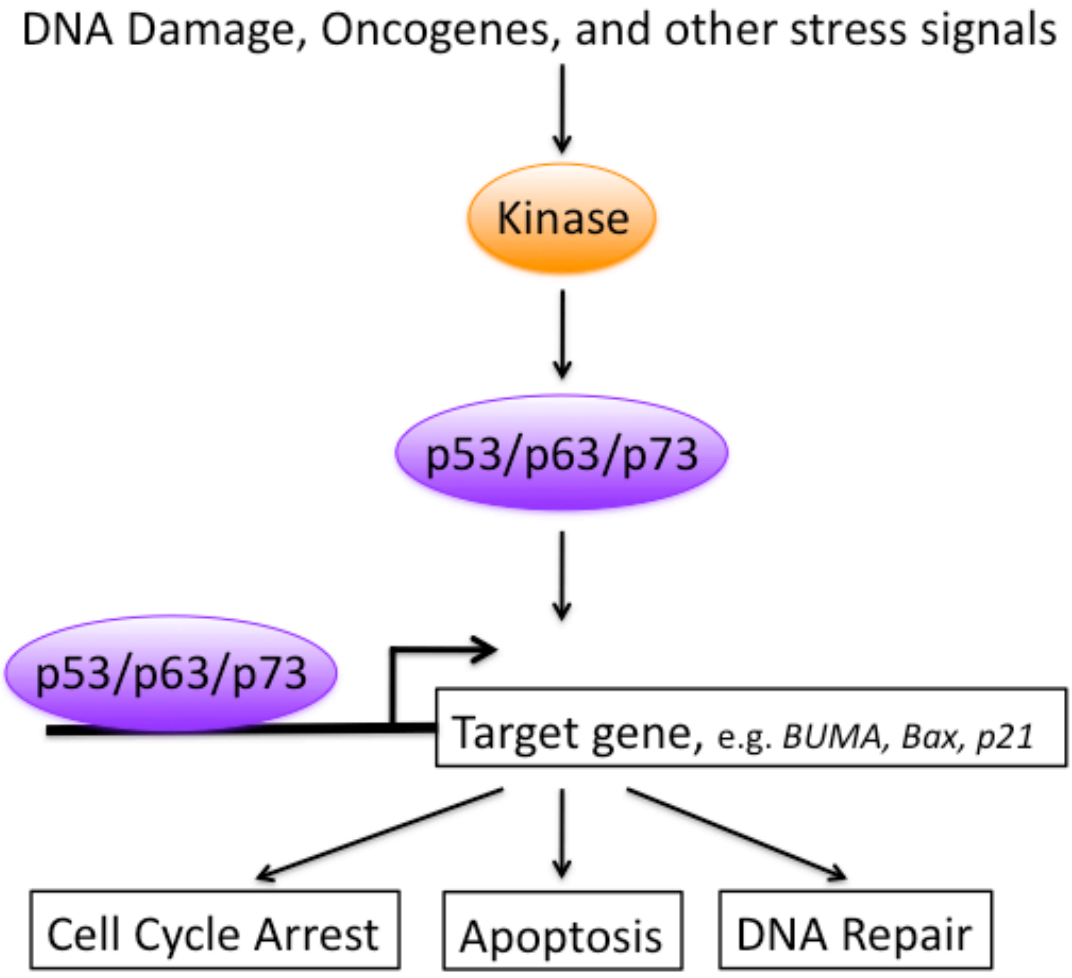

Figure 1.2. The p53 protein family pathway. Upon DNA damage or cellular stress, the p53 family proteins are activated by kinases through post-translational modification. The activated p53 family proteins bind to the promoters of the target genes and activate the transcription of the target genes to induce cell cycle arrest, apoptosis, and DNA repair.

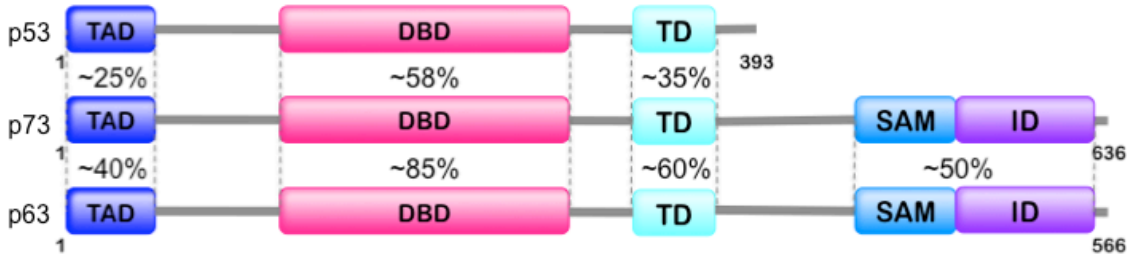

Figure 1.3. Structural comparison between the p53 family proteins. The p53 family proteins are conserved in transactivation domain (TAD), DNA-binding domain (DBD), and tetramerization domain (TD). p63 and p73 have an additional C-terminal domain including sterile alpha motif domain (SAM) and inhibitory domain (ID). The percentage of similarity of each domain between p73/p53 and p73/p63 is indicated.

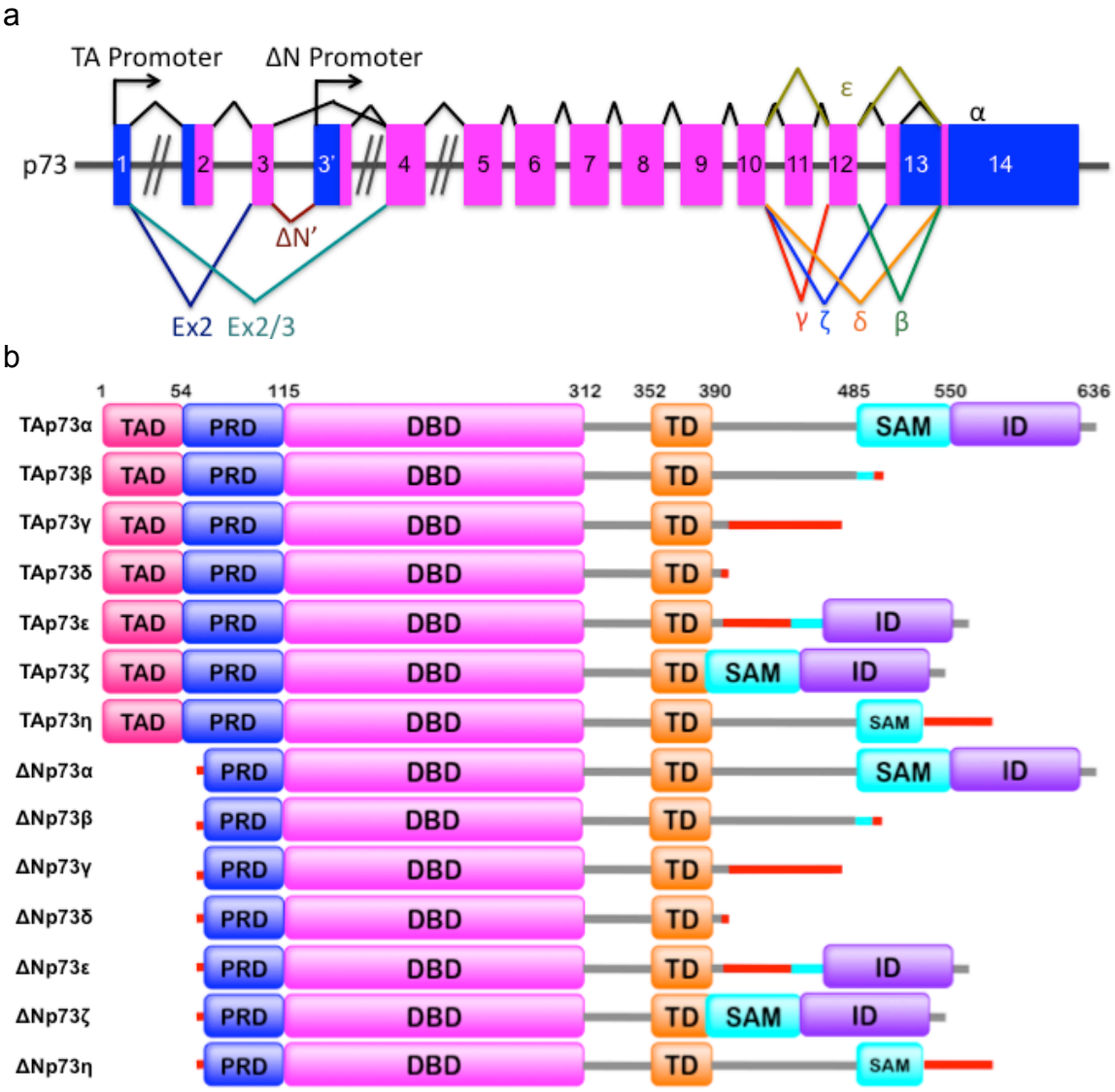

Figure 1.4. The human *TP73* gene structure and domain organization of p73 isoforms. a) The gene structure of human p73. p73 isoforms are generated from alternative splicing (α, β, γ, δ, ε, ζ, η) and alternative promoters (TA promoter and ΔN promoter). b) Schematic representation of TAp73 and ΔNp73. TAp73 and ΔNp73 are generated from different promoters which have opposite functions. TAp73 is transcriptional activator while ΔNp73 is transcriptional inhibitor. Both isoforms exist in different forms of splicing, which have different transcriptional activities. The lines in red indicated the regions that are different from the full-length p73.

G. References

Avantaggiati, M.L., Ogryzko, V., Gardner, K., Giordano, A., Levine, A.S., and Kelly, K. (1997). Recruitment of p300/CBP in p53-dependent signal pathways. Cell *89*, 1175-1184.

Bell, H.S., and Ryan, K.M. (2007). Targeting the p53 family for cancer therapy: 'big brother' joins the fight. Cell Cycle *6*, 1995-2000.

Chen, Y., Dey, R., and Chen, L. (2010). Crystal structure of the p53 core domain bound to a full consensus site as a self-assembled tetramer. Structure *18*, 246-256.

Chene, P. (2001). The role of tetramerization in p53 function. Oncogene *20*, 2611-2617.

Cho, Y., Gorina, S., Jeffrey, P.D., and Pavletich, N.P. (1994). Crystal structure of a p53 tumor suppressor-DNA complex: understanding tumorigenic mutations. Science *265*, 346-355.

Conaway, J.W., Florens, L., Sato, S., Tomomori-Sato, C., Parmely, T.J., Yao, T., Swanson, S.K., Banks, C.A., Washburn, M.P., and Conaway, R.C. (2005). The mammalian Mediator complex. FEBS Lett *579*, 904-908.

Coutandin, D., Lohr, F., Niesen, F.H., Ikeya, T., Weber, T.A., Schafer, B., Zielonka, E.M., Bullock, A.N., Yang, A., Guntert, P.*, et al.* (2009). Conformational stability and activity of p73 require a second helix in the tetramerization domain. Cell death and differentiation *16*, 1582-1589.

De Laurenzi, V., Costanzo, A., Barcaroli, D., Terrinoni, A., Falco, M., Annicchiarico-Petruzzelli, M., Levrero, M., and Melino, G. (1998). Two new p73 splice variants, gamma and delta, with different transcriptional activity. The Journal of experimental medicine *188*, 1763-1768.

De Laurenzi, V.D., Catani, M.V., Terrinoni, A., Corazzari, M., Melino, G., Costanzo, A., Levrero, M., and Knight, R.A. (1999). Additional complexity in p73: induction by mitogens in lymphoid cells and identification of two new splicing variants epsilon and zeta. Cell death and differentiation *6*, 389-390.

el-Deiry, W.S., Kern, S.E., Pietenpol, J.A., Kinzler, K.W., and Vogelstein, B. (1992). Definition of a consensus binding site for p53. Nature genetics *1*, 45-49.
Fourel, G., Magdinier, F., and Gilson, E. (2004). Insulator dynamics and the setting of chromatin domains. Bioessays *26*, 523-532.

Gressner, O., Schilling, T., Lorenz, K., Schulze Schleithoff, E., Koch, A., Schulze-Bergkamen, H., Lena, A.M., Candi, E., Terrinoni, A., Catani, M.V.*, et al.* (2005). TAp63alpha induces apoptosis by activating signaling via death receptors and mitochondria. Embo J *24*, 2458-2471.

Grob, T.J., Novak, U., Maisse, C., Barcaroli, D., Luthi, A.U., Pirnia, F., Hugli, B., Graber, H.U., De Laurenzi, V., Fey, M.F.*, et al.* (2001). Human delta Np73 regulates a dominant negative feedback loop for TAp73 and p53. Cell death and differentiation *8*, 1213-1223.

Haupt, Y., Maya, R., Kazaz, A., and Oren, M. (1997). Mdm2 promotes the rapid degradation of p53. Nature *387*, 296-299.

Ho, W.C., Fitzgerald, M.X., and Marmorstein, R. (2006). Structure of the p53 core domain dimer bound to DNA. J Biol Chem *281*, 20494-20502.

Hollstein, M., Rice, K., Greenblatt, M.S., Soussi, T., Fuchs, R., Sorlie, T., Hovig, E., Smith-Sorensen, B., Montesano, R., and Harris, C.C. (1994). Database of p53 gene somatic mutations in human tumors and cell lines. Nucleic acids research *22*, 3551-3555.

Hollstein, M., Sidransky, D., Vogelstein, B., and Harris, C.C. (1991). p53 mutations in human cancers. Science *253*, 49-53.

Irwin, M., Marin, M.C., Phillips, A.C., Seelan, R.S., Smith, D.I., Liu, W., Flores, E.R., Tsai, K.Y., Jacks, T., Vousden, K.H.*, et al.* (2000). Role for the p53 homologue p73 in E2F-1-induced apoptosis. Nature *407*, 645-648.

Ishimoto, O., Kawahara, C., Enjo, K., Obinata, M., Nukiwa, T., and Ikawa, S. (2002). Possible oncogenic potential of DeltaNp73: a newly identified isoform of human p73. Cancer research *62*, 636-641.

Kaghad, M., Bonnet, H., Yang, A., Creancier, L., Biscan, J.C., Valent, A., Minty, A., Chalon, P., Lelias, J.M., Dumont, X.*, et al.* (1997). Monoallelically expressed gene related to p53 at 1p36, a region frequently deleted in neuroblastoma and other human cancers. Cell *90*, 809-819.

Kim, E., and Deppert, W. (2006). The versatile interactions of p53 with DNA: when flexibility serves specificity. Cell death and differentiation *13*, 885-889.

Kitayner, M., Rozenberg, H., Kessler, N., Rabinovich, D., Shaulov, L., Haran, T.E., and Shakked, Z. (2006). Structural basis of DNA recognition by p53 tetramers. Mol Cell *22*, 741-753.

Kitayner, M., Rozenberg, H., Rohs, R., Suad, O., Rabinovich, D., Honig, B., and Shakked, Z. (2010). Diversity in DNA recognition by p53 revealed by crystal structures with Hoogsteen base pairs. Nat Struct Mol Biol *17*, 423-429.

Kubbutat, M.H., Jones, S.N., and Vousden, K.H. (1997). Regulation of p53 stability by Mdm2. Nature *387*, 299-303.

Lane, D.P., and Crawford, L.V. (1979). T antigen is bound to a host protein in SV40-transformed cells. Nature *278*, 261-263.

Lefstin, J.A., and Yamamoto, K.R. (1998). Allosteric effects of DNA on transcriptional regulators. Nature *392*, 885-888.

Linzer, D.I., and Levine, A.J. (1979). Characterization of a 54K dalton cellular SV40 tumor antigen present in SV40-transformed cells and uninfected embryonal carcinoma cells. Cell *17*, 43-52.

Liu, G., and Chen, X. (2005). The C-terminal sterile alpha motif and the extreme C terminus regulate the transcriptional activity of the alpha isoform of p73. J Biol Chem *280*, 20111-20119.

Liu, Y., and Kulesz-Martin, M.F. (2006). Sliding into home: facilitated p53 search for targets by the basic DNA binding domain. Cell death and differentiation *13*, 881-884.

Lokshin, M., Li, Y., Gaiddon, C., and Prives, C. (2007). p53 and p73 display common and distinct requirements for sequence specific binding to DNA. Nucleic acids research *35*, 340-352.

Malecka, K.A., Ho, W.C., and Marmorstein, R. (2009). Crystal structure of a p53 core tetramer bound to DNA. Oncogene *28*, 325-333.

Malik, S., and Roeder, R.G. (2005). Dynamic regulation of pol II transcription by the mammalian Mediator complex. Trends Biochem Sci *30*, 256-263.

Maston, G.A., Evans, S.K., and Green, M.R. (2006). Transcriptional regulatory elements in the human genome. Annu Rev Genomics Hum Genet *7*, 29-59.

Melino, G., De Laurenzi, V., and Vousden, K.H. (2002). p73: Friend or foe in tumorigenesis. Nature reviews Cancer *2*, 605-615.

Melino, G., Lu, X., Gasco, M., Crook, T., and Knight, R.A. (2003). Functional regulation of p73 and p63: development and cancer. Trends Biochem Sci *28*, 663-670.

Petty, T.J., Emamzadah, S., Costantino, L., Petkova, I., Stavridi, E.S., Saven, J.G., Vauthey, E., and Halazonetis, T.D. (2011). An induced fit mechanism regulates p53 DNA binding kinetics to confer sequence specificity. Embo J *30*, 2167-2176.

Pietsch, E.C., Sykes, S.M., McMahon, S.B., and Murphy, M.E. (2008). The p53 family and programmed cell death. Oncogene *27*, 6507-6521.

Pozniak, C.D., Radinovic, S., Yang, A., McKeon, F., Kaplan, D.R., and Miller, F.D. (2000). An anti-apoptotic role for the p53 family member, p73, during developmental neuron death. Science *289*, 304-306.
Ptashne, M., and Gann, A. (1997). Transcriptional activation by recruitment. Nature *386*, 569-577.

Remenyi, A., Scholer, H.R., and Wilmanns, M. (2004). Combinatorial control of gene expression. Nat Struct Mol Biol *11*, 812-815.

Schultz, J., Ponting, C.P., Hofmann, K., and Bork, P. (1997). SAM as a protein interaction domain involved in developmental regulation. Protein science : a publication of the Protein Society *6*, 249-253.

Scully, K.M., Jacobson, E.M., Jepsen, K., Lunyak, V., Viadiu, H., Carriere, C., Rose, D.W., Hooshmand, F., Aggarwal, A.K., and Rosenfeld, M.G. (2000). Allosteric effects of Pit-1 DNA sites on long-term repression in cell type specification. Science *290*, 1127-1131.

Serber, Z., Lai, H.C., Yang, A., Ou, H.D., Sigal, M.S., Kelly, A.E., Darimont, B.D., Duijf, P.H., Van Bokhoven, H., McKeon, F*., et al.* (2002). A C-terminal inhibitory domain controls the activity of p63 by an intramolecular mechanism. Mol Cell Biol *22*, 8601-8611.

Shaw, P., Bovey, R., Tardy, S., Sahli, R., Sordat, B., and Costa, J. (1992). Induction of apoptosis by wild-type p53 in a human colon tumor-derived cell line. Proc Natl Acad Sci U S A *89*, 4495-4499.

Smeenk, L., van Heeringen, S.J., Koeppel, M., van Driel, M.A., Bartels, S.J., Akkers, R.C., Denissov, S., Stunnenberg, H.G., and Lohrum, M. (2008). Characterization of genome-wide p53-binding sites upon stress response. Nucleic acids research *36*, 3639-3654.

Stiewe, T., Theseling, C.C., and Putzer, B.M. (2002). Transactivation-deficient Delta TA-p73 inhibits p53 by direct competition for DNA binding: implications for tumorigenesis. J Biol Chem *277*, 14177-14185.

Tomasini, R., Mak, T.W., and Melino, G. (2008). The impact of p53 and p73 on aneuploidy and cancer. Trends in cell biology *18*, 244-252.

Viadiu, H. (2008). Molecular architecture of tumor suppressor p53. Current topics in medicinal chemistry *8*, 1327-1334.

Yang, A., Kaghad, M., Wang, Y., Gillett, E., Fleming, M.D., Dotsch, V., Andrews, N.C., Caput, D., and McKeon, F. (1998). p63, a p53 homolog at 3q27-29, encodes multiple products with transactivating, death-inducing, and dominant-negative activities. Mol Cell *2*, 305-316.

Yang, A., Schweitzer, R., Sun, D., Kaghad, M., Walker, N., Bronson, R.T., Tabin, C., Sharpe, A., Caput, D., Crum, C*., et al.* (1999). p63 is essential for regenerative proliferation in limb, craniofacial and epithelial development. Nature *398*, 714-718.

Yang, A., Walker, N., Bronson, R., Kaghad, M., Oosterwegel, M., Bonnin, J., Vagner, C., Bonnet, H., Dikkes, P., Sharpe, A*., et al.* (2000). p73-deficient mice have neurological, pheromonal and inflammatory defects but lack spontaneous tumours. Nature *404*, 99-103.

Yonish-Rouach, E., Resnitzky, D., Lotem, J., Sachs, L., Kimchi, A., and Oren, M. (1991). Wild-type p53 induces apoptosis of myeloid leukaemic cells that is inhibited by interleukin-6. Nature *352*, 345-347.

Zeng, X., Chen, L., Jost, C.A., Maya, R., Keller, D., Wang, X., Kaelin, W.G., Jr., Oren, M., Chen, J., and Lu, H. (1999). MDM2 suppresses p73 function without promoting p73 degradation. Mol Cell Biol *19*, 3257-3266.

Chapter 2

Minimum DNA Length Required for p73 DBD Binding

A. Introduction

The p53 consensus sequence was first identified using cyclic amplification and selection of targets (CASTing) and alignment of genomic clones that bound to p53 *in vitro* (el-Deiry et al., 1992; Funk et al., 1992). Later, this consensus sequence has been confirmed by chromatin immunoprecipitation (ChIP) with paired-end ditag (PET), and the p53 transcription function with this consensus sequence was verified using luciferase reporter assay (Wang et al., 2009; Wei et al., 2006). Moreover, p73 target genes were identified by DNA microarray and ChIP analyses. The results have shown that p73 binds to the same consensus sequence as p53 (Fontemaggi et al., 2002).

The canonical p53 response elements (REs) are 20 bp DNA sequences that consist of two 10 bp half-sites with a consensus sequence of Pu1-Pu2-Pu3-C4-A5/T5-T5/A5-G4-Py3-Py2-Py1 (Pu=purine, and Py=pyrimidine) (el-Deiry et al., 1992; Funk et al., 1992). Upon DNA damage or cellular stresses, the p53 family proteins recognize these sites and bind to specific DNA REs located within the promoter/enhancer region. Once bound to the RE, they promote the activation of target genes that are involved in the cell cycle arrest or apoptosis (Pietsch et al., 2008).

In the cell, the p53 family proteins function as tetramer. The crystal structures have shown that p53 DBD is bound to canonical DNA REs as a tetramer. One monomer binds to a 5 bp DNA, which is known as a quarter-site RE; two monomers bind to a 10 bp half-site as a dimer; and two dimers bind to a full-site as a tetramer (Chen et al., 2010; Cho et al., 1994; Ho et al., 2006;

Kitayner et al., 2006; Kitayner et al., 2010; Malecka et al., 2009; Petty et al., 2011).

From previous structural studies, it is known that p53 DBD makes direct contacts with the central Pu3-C4-A5/T5-T5/A5-G4-Py3 motif of a canonical half-site. The nucleotides at positions 1 and 2 are involved in phosphate backbone contact (Cho et al., 1994). In addition, alignment of all the functional p53 REs that were validated experimentally have shown that the central C4-A5/T5-T5/A5-G4 motif was the most conserved motif, and the nucleotides C and G are the most crucial nucleotides within the consensus sequence (Riley et al., 2008). To determine whether p73 recognizes DNA using a similar mechanism as p53, I would like to determine the minimum length of a half-site that is required for p73 DBD to bind as a dimer. In order to achieve this goal, I have carried out DNA binding studies using analytical ultracentrifugation (AUC) and fluorescence anisotropy.

B. Materials and methods

1. Cloning

The DNA sequence of human p73 DBD encoding amino acid residues 115-312 was amplified by PCR using a template of a full-length p73. The PCR product was cloned into the pET28a bacterial expression vector (Novagen) using EcoRI and HindIII restriction sites.

2. Protein Expression and Purification

The recombinant plasmid of p73 DBD was transformed into *E. coli* BL21/DE3 cells. The cells were expressed in LB medium containing 30 μg/mL kanamycin at 37 °C until OD_{600nm} reached 0.6-0.8, and the cells were induced by 0.5 mM isopropyl-β-D-thiogalactopyranoside (IPTG) at 25 °C for 4 hours. The cells were harvested by centrifugation and the cell pellets were resuspended in a buffer containing 500 mM NaCl, 20 mM sodium citrate (pH 6.1), and 10 μM $ZnCl_2$. The cells were then lysed in French press with addition of 1 mM phenylmethanesulfonylfluoride protease inhibitor (PMSF). The cell lysate was centrifuged by ultracentrifugation at 30,000 rpm, 4°C for 30 minutes. The soluble fraction was incubated with 2 mL of Ni-NTA resin (QIAGEN) at 4 °C for 30 minutes and transferred to a gravity column. The resin was first washed with 100 mL of the buffer and then 50 mL of the buffer with 20 mM imidazole. The protein was eluted with 300 mM imidazole. The protein purified from the affinity column was analyzed by SDS-PAGE (15%, w/v) followed by Coomassie staining and western blotting using anti-His antibody (Roche, 0490527001). The protein was

then further purified by gel filtration chromatography using superdex-200 column. The column was equilibrated using a buffer with 100 mM NaCl, 10 mM sodium citrate (pH 6.1), 5 mM DTT, and 5 μM $ZnCl_2$. A sample of p73 DBD was loaded onto the superdex-200 column at room temperature at a flow rate of 0.5 mL/min. The absorbance was recorded at 280nm (Figure 2.4). The purified protein was analyzed by SDS-PAGE (15 %, w/v) followed by Coomassie staining and western blotting using anti-His antibody (Roche, 0490527001).

4. Analytical ultracentrifugation (AUC)

Sedimentation velocity experiments were performed in 100 mM NaCl, 10 mM sodium citrate (pH 6.1), 5 mM DTT, and 5 μM $ZnCl_2$ using Beckman Optima XL-I analytical ultracentrifuge with an An-60 Ti rotor. For the protein experiment, 400 μL of buffer and 416 μM p73 DBD were loaded into a double-sector centerpiece. The experiment was carried out at 50,000 rpm, 20 °C, and the radial scans were collected at 280 nm. For the fluorescence experiments, 400 μL of buffer and protein:DNA complex containing 64.5 μM of p73 DBD and 3-3.4 μM of 5'-fluorescein-labeled dsDNA (Table 2.1) were loaded into double sector centerpieces. The experiments were carried out at 50,000 rpm, 20 °C, and the radial scans were collected at 488 nm. The collected data were analyzed using SEDFIT software to calculate c(s) distributions (Lebowitz et al., 2002). SEDNTERP software was used to calculate the partial specific volume, buffer viscosity and buffer density (Laue et al., 1992).

5. Fluorescence Anisotropy

Fluorescence anisotropy experiments were performed in 100 mM NaCl, 10 mM sodium citrate (pH 6.1), 5 mM DTT, and 5 μM $ZnCl_2$. p73 DBD was serially diluted from 160 μM to 1 nM and there were a total of 17 tubes prepared with different concentrations at a final volume of 500 μL. The 5'-fluorescein-labeled dsDNA (Table 2.1) was added to each tube to a final concentration of 5 nM. The tubes were incubated on ice for 45 minutes, and the fluorescence intensity of each tube was measured using Hitachi F-2000 fluorescence spectrophotometer with excitation and emission wavelengths of 494 nm and 521 nm, respectively. The fluorescence anisotropy data was analyzed using non-linear regression curve with the Prism graphical software.

Table 2.1. Sequences of 6-22 bp fluorescein-labeled DNA. The sequences of fluorescein-labeled DNA that were used in the AUC and fluorescence anisotropy experiments.

Length of the DNA	Sequence
6 bp	5′-FAM/GCATGC-3′ 3′-CGTACG/FAM-5′
8 bp	5′-FAM/GGCATGCC-3′ 3′-CCGTACGG/FAM-5′
10 bp	5′-FAM/GGGCATGCCC-3′ 3′-CCCGTACGGG/FAM-5′
12 bp	5′-FAM/TGGGCATGCCCA-3′ 3′-ACCCGTACGGGT/FAM-5′
22 bp	5′-FAM/CGGGCATGCCCGGGCATGCCCG-3′ 3′-GCCCGTACGGGCCCGTACGGGC/FAM-5′

C. Results

1. Purification of 8His-p73 DBD (115-312)

8His-p73 DBD (115-312) was purified using nickel affinity chromatography (Figure 2.1); followed by gel filtration chromatography. The purity of the protein is shown in Figure 2.2.

2. p73 DBD forms oligomer in the presence of DNA

From gel filtration chromatography, it was confirmed that p73 DBD is presented as a monomer in solution. In order to determine the oligomeric state of p73 DBD in the presence of DNA, I carried out DNA binding studies of p73 DBD using AUC. In the sedimentation velocity experiments, I have determined the sedimentation coefficients of p73 DBD in complex with 5'-fluorescence labeled DNAs: 12 bp 5'-T**GGGCATGCCC**A-3' that contains a half-site RE and 22 bp 5'-C**GGGCATGCCCGGGCATGCCC**G-3' that contains a full-site RE. In AUC experiments, when p73 DBD is present as a monomer in the absence of DNA, the sedimentation coefficient was determined to be 2.10 S. However, the oligomeric states of p73 DBD as well as the sedimentation coefficients have changed upon the presence of DNA with different lengths. The result showed that upon binding to 12 bp DNA, p73 DBD became a dimer with a sedimentation coefficient of 4.29 S. More importantly, p73 DBD became a tetramer in the presence of 22 bp DNA and with a sedimentation coefficient of 6.68 S (Figure 2.3). These results have suggested that the p73 DBD oligomerize upon DNA

binding; and its oligomerization state is depended on the length of DNA and the number of its binding site.

3. A 6 bp half-site is sufficient for the p73 DBD to bind as a dimer, but 8 bp half-site is required to have a binding affinity comparable to the original 12 bp half-site

From the AUC experiment, p73 DBD was shown to bind to a 10 bp half-site RE as a dimer. To determine the minimum length of half-site that is required to initiate p73 DBD dimerization, I have utilized four different lengths of 5'-fluorescence labeled DNAs: 6 bp half-site 5'-**GCATGC**-3', 8 bp half-site 5'**GGCA-TGCC**-3', 10 bp half-site 5'-**GGGCATGCCC**-3' and 12 bp 5'-T**GGGCATGCCC**A-3' that contains 10 bp half-site. For this experiment, I used AUC to understand the oligomeric state of p73 DBD:DNA complexes. The sedimentation coefficient distribution in Figure 2.4 shows that p73 DBD bound to all 6-12 bp DNAs as dimers with sedimentation coefficients between 3.28 S to 4.29 S. As the length of the half-site decreases, the sedimentation coefficient also decreases. I also carried out fluorescence anisotropy experiments to determine the binding affinity of p73 DBD to those DNAs. The results of fluorescence anisotropy in Figure 2.5 shows the dissociation constant (K_d) of p73 DBD for 12 bp DNA to be 2.83 μM. The K_d were 5.97 μM and 12.06 μM for 10 bp and 8 bp DNA respectively, which were slightly larger than the K_d for 12 bp. However, when the length of the half-site decreased to 6 bp, the K_d was larger than 100 μM. Although p73 DBD can bind to 6 bp half-site as a dimer, 8 bp half-site is required for p73 DBD to bind

with a binding affinity comparable to the original 12 bp half-site. Because p73 DBD has the strongest binding affinity with 12 bp DNA, the later DNA binding experiments were performed with 12 bp DNAs.

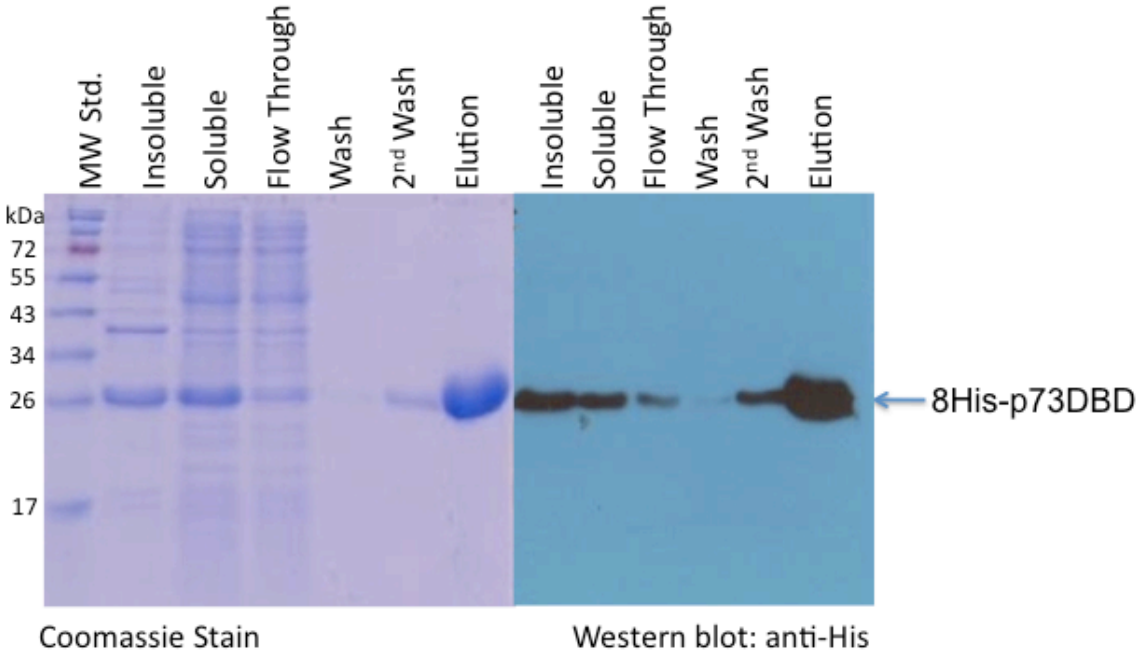

Figure 2.1. Purification of recombinant human 8His-p73 DBD (115-312) using Ni affinity chromatography. Coomassie stain (left) and western blot (right) of 15 % SDS-PAGE analysis have showed p73 DBD migrated at ~26 kDa.

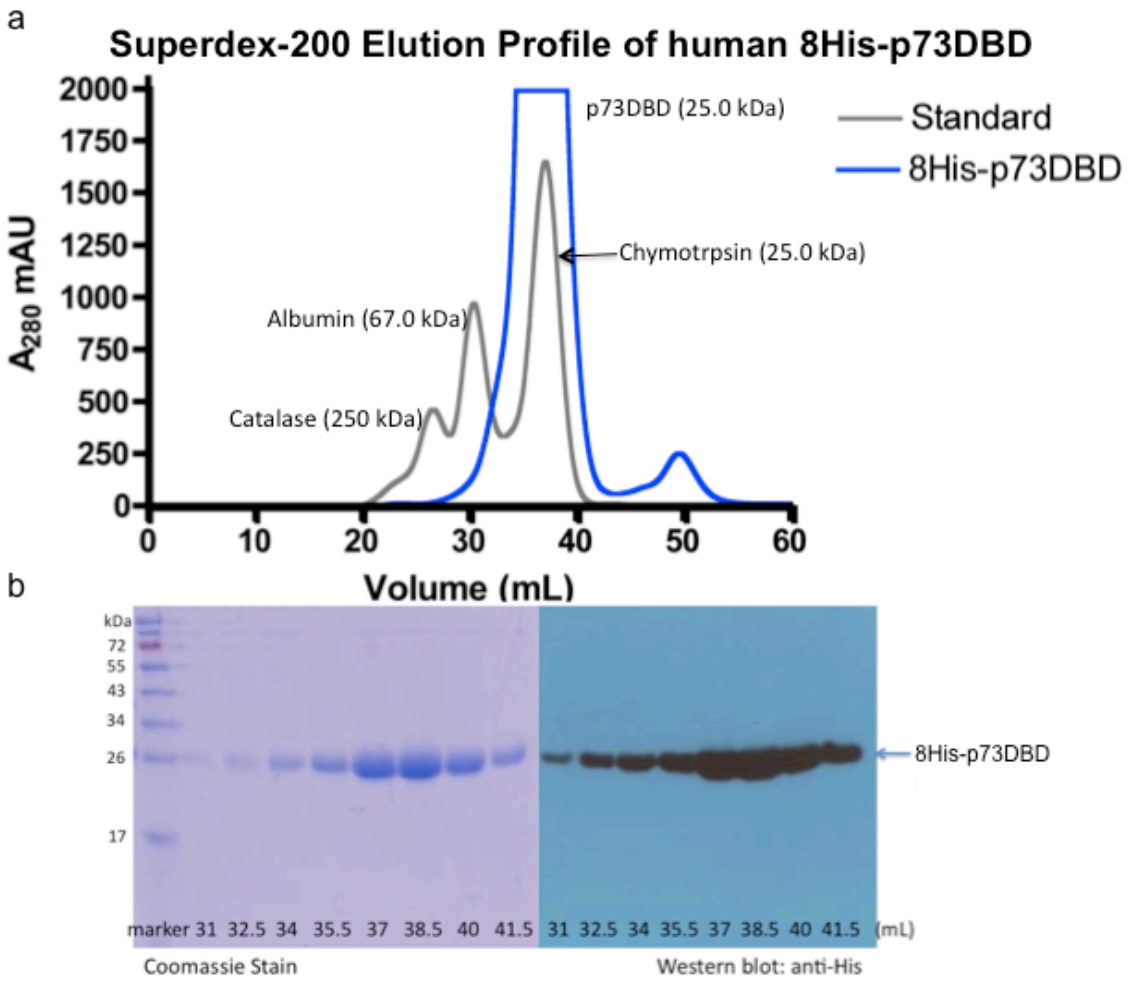

Figure 2.2. Purification of recombinant human 8His-p73 DBD (115-312) using gel filtration chromatography. a) Sperdex-200 gel filtration chromatography elution profile has showed a single peak of p73 DBD. b) 15 % SDS-PAGE analysis of fractions from Superdex-200 gel filtration chromatography.

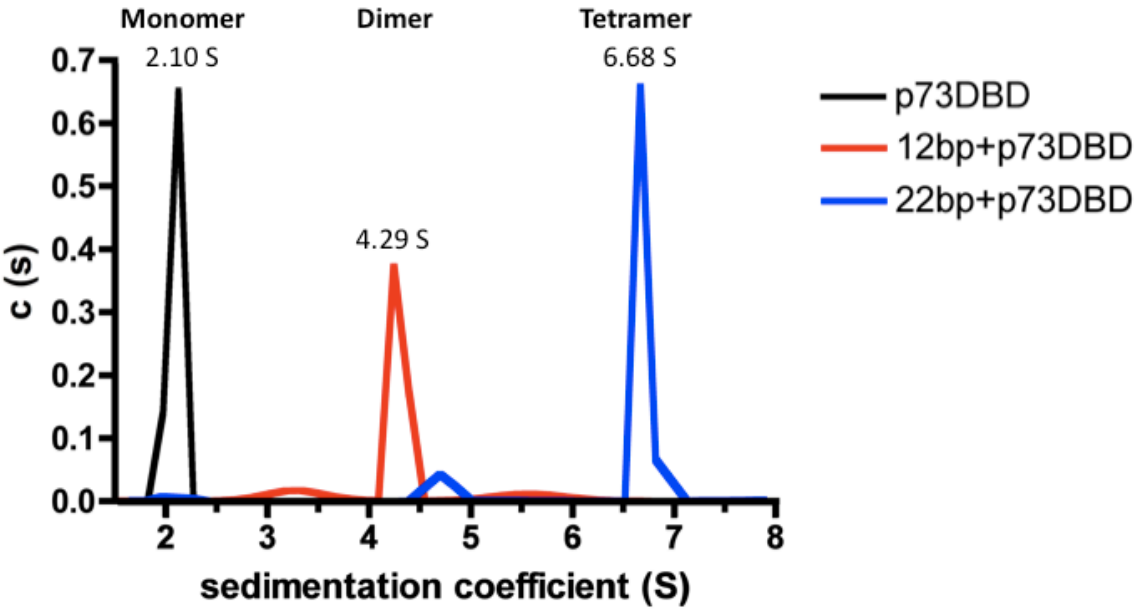

Figure 2.3. Sedimentation coefficient distribution of the oligomeric state of 8His-p73 DBD.

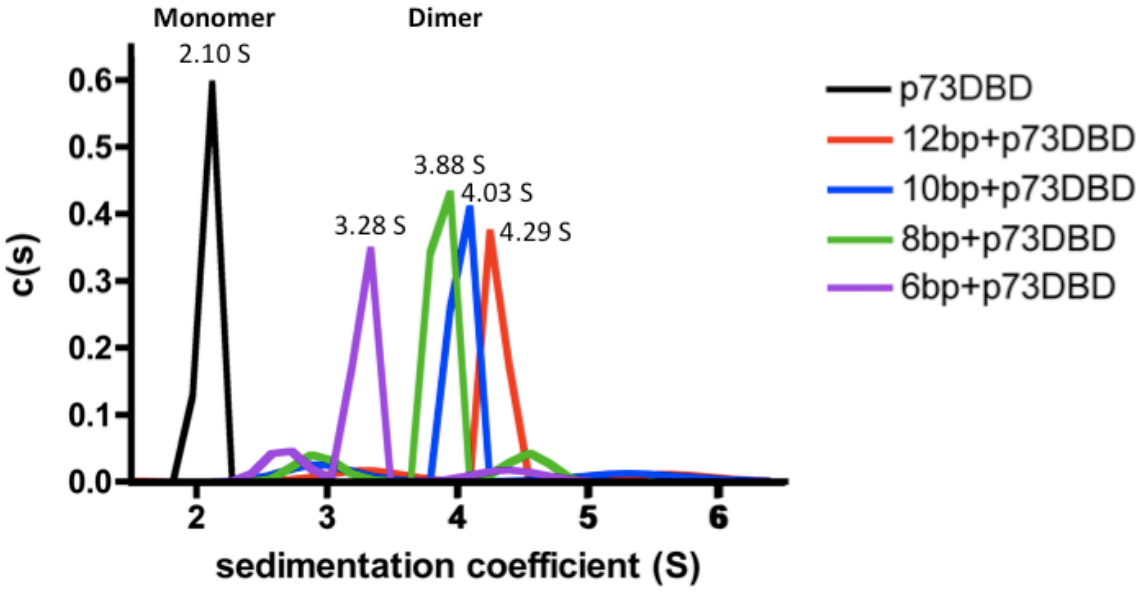

Figure 2.4. Sedimentation coefficient distribution of 8His-p73 DBD with different length of DNAs.

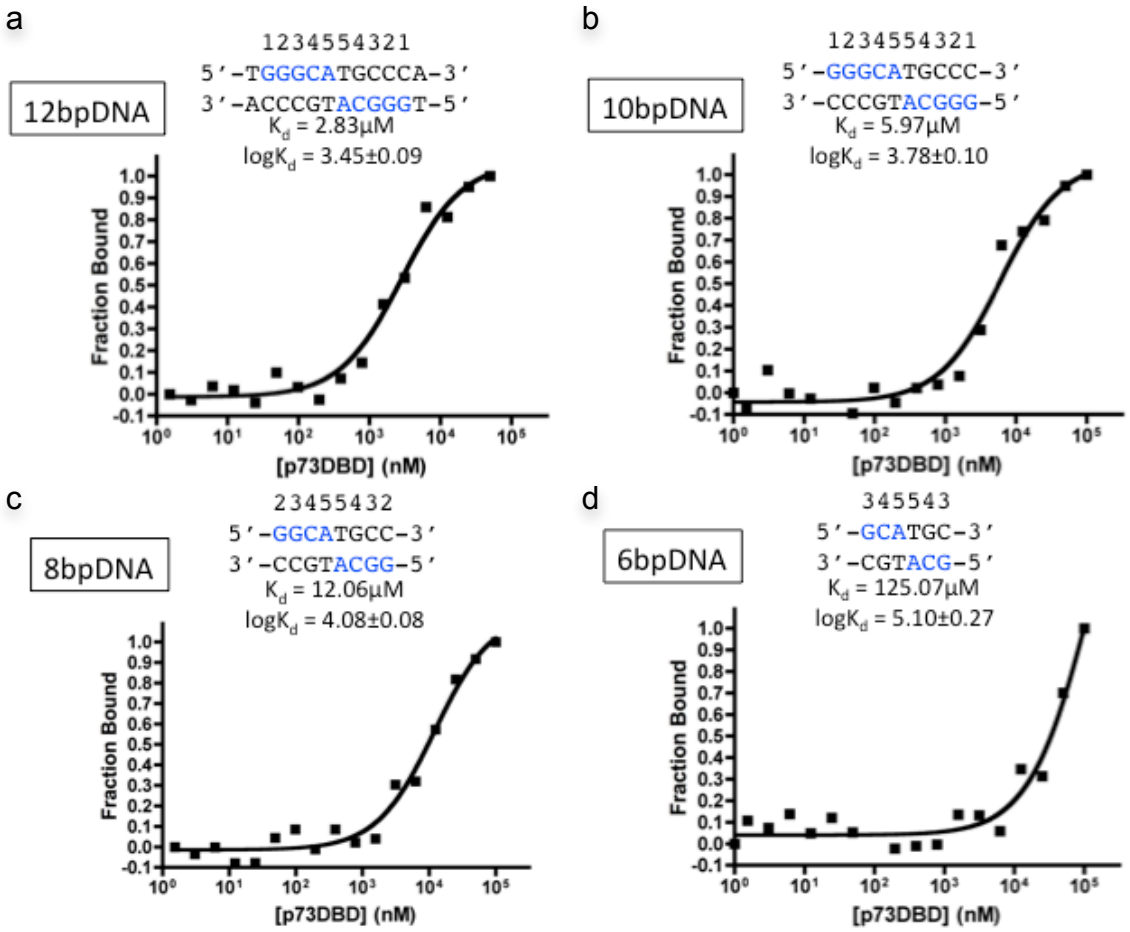

Figure 2.5. Fluorescence Anisotropy of 8His-p73 DBD with different length of DNAs. The dissociation constant (K_d) of p73 DBD with a) 12 bp DNA is 2.825 μM; b) 10 bp DNA is 5.974 μM; c) 8 bp DNA is 12.06 μM; and d) 6 bp DNA is 125.1 μM.

D. Discussion

Both gel filtration chromatography and sedimentation velocity experiments have indicated that p73 DBD appears as a monomer in the absence of DNA (Figure 2.2 and 2.3). Upon DNA binding, p73 DBD oligomerizes and its oligomerization states are depended on the length of DNA and the number of consensus binding sites. p73 DBD binds to a 12 bp oligonucleotide that contains a half-site RE as a dimer and a 22 bp oligonucleotide with a full-site RE as a tetramer (Figure 2.3). Based on sedimentation velocity experiments, p73 DBD binds to a 6 bp half-site (Pu3-C4-A5/T5-T5/A5-G4-Py3) as a dimer; however, the binding affinity drops significantly (K_d is ~125 μM) (Figure 2.4 and 2.5). As the length of the half-site increased to 8, 10, and 12 bp half-site, the binding affinities drastically increase (K_d is 3-12 μM) (Figure 2.5). As seen from the crystal structures of DNA complex with p73 DBD and p53 DBD, the interactions of protein with DNA bp at position 2 and 3 are significant for binding (Cho et al., 1994). Therefore, the decrease in binding affinity is due to the loss of those interactions with the bp. From the sedimentation velocity and fluorescence anisotropy experiments, I can conclude that the p73 DBD binds to a minimum 6 bp half-site as dimer; however, it cannot form a functional dimer or tetramer with 6 bp half-site. In order to form a functional dimer or tetramer, it requires a minimum of 8bp half-site.

E. References

Chen, Y., Dey, R., and Chen, L. (2010). Crystal structure of the p53 core domain bound to a full consensus site as a self-assembled tetramer. Structure *18*, 246-256.

Cho, Y., Gorina, S., Jeffrey, P.D., and Pavletich, N.P. (1994). Crystal structure of a p53 tumor suppressor-DNA complex: understanding tumorigenic mutations. Science *265*, 346-355.

el-Deiry, W.S., Kern, S.E., Pietenpol, J.A., Kinzler, K.W., and Vogelstein, B. (1992). Definition of a consensus binding site for p53. Nature genetics *1*, 45-49.

Fontemaggi, G., Kela, I., Amariglio, N., Rechavi, G., Krishnamurthy, J., Strano, S., Sacchi, A., Givol, D., and Blandino, G. (2002). Identification of direct p73 target genes combining DNA microarray and chromatin immunoprecipitation analyses. J Biol Chem *277*, 43359-43368.

Funk, W.D., Pak, D.T., Karas, R.H., Wright, W.E., and Shay, J.W. (1992). A transcriptionally active DNA-binding site for human p53 protein complexes. Mol Cell Biol *12*, 2866-2871.

Ho, W.C., Fitzgerald, M.X., and Marmorstein, R. (2006). Structure of the p53 core domain dimer bound to DNA. J Biol Chem *281*, 20494-20502.

Kitayner, M., Rozenberg, H., Kessler, N., Rabinovich, D., Shaulov, L., Haran, T.E., and Shakked, Z. (2006). Structural basis of DNA recognition by p53 tetramers. Mol Cell *22*, 741-753.

Kitayner, M., Rozenberg, H., Rohs, R., Suad, O., Rabinovich, D., Honig, B., and Shakked, Z. (2010). Diversity in DNA recognition by p53 revealed by crystal structures with Hoogsteen base pairs. Nat Struct Mol Biol *17*, 423-429.

Laue, T.M., Shah, B.D., Ridgeway, T.M., and Pelletier, S.L. (1992). Computer-Aided Interpreation of Analytical Sedimentation Data for Proteins. In Analytical Ultracentrifugation in Biochemistry and Polymer Science, S.E. Harding, A.J. Rowe, and J.C. Horton, eds. (Royal Society of Chemistry).

Lebowitz, J., Lewis, M.S., and Schuck, P. (2002). Modern analytical ultracentrifugation in protein science: a tutorial review. Protein science : a publication of the Protein Society *11*, 2067-2079.

Malecka, K.A., Ho, W.C., and Marmorstein, R. (2009). Crystal structure of a p53 core tetramer bound to DNA. Oncogene *28*, 325-333.

Petty, T.J., Emamzadah, S., Costantino, L., Petkova, I., Stavridi, E.S., Saven, J.G., Vauthey, E., and Halazonetis, T.D. (2011). An induced fit mechanism regulates p53 DNA binding kinetics to confer sequence specificity. Embo J *30*, 2167-2176.

Pietsch, E.C., Sykes, S.M., McMahon, S.B., and Murphy, M.E. (2008). The p53 family and programmed cell death. Oncogene *27*, 6507-6521.

Riley, T., Sontag, E., Chen, P., and Levine, A. (2008). Transcriptional control of human p53-regulated genes. Nature reviews Molecular cell biology *9*, 402-412.

Wang, B., Xiao, Z., and Ren, E.C. (2009). Redefining the p53 response element. Proc Natl Acad Sci U S A *106*, 14373-14378.

Wei, C.L., Wu, Q., Vega, V.B., Chiu, K.P., Ng, P., Zhang, T., Shahab, A., Yong, H.C., Fu, Y., Weng, Z.*, et al.* (2006). A global map of p53 transcription-factor binding sites in the human genome. Cell *124*, 207-219.

Chapter 3

DNA Binding Specificity of p73 DBD

A. Introduction

The DNA-binding domain (DBD) is highly conserved within the p53 protein family. The sequence alignment between the members of the family shows that p73 DBD has 58% similarity with p53 DBD and 85% with p63 DBD (Figure 3.1). Besides the high sequence similarity of the p53 family proteins, the residues involved in DNA binding are also conserved. The overall structure of DBD forms an immunoglobulin-like β-sandwich fold. The structure of p73 DBD monomer consists of 11 β-strands (S1-S10), 2 alpha-helices (H1 and H2), and 3 loops (L1-L3) (Figure 3.2). The helix H1 and loop L3 are involved in interaction with Zn^{2+} ion, which is crucial for dimerization and DNA binding, while L1, L3, S10, and H2 involves in DNA binding. Moreover, the crystal structures of the p53 family proteins bound to DNA have shown that the interactions between protein and DNA are the same (Chen et al., 2011; Cho et al., 1994).

The quarter-site of the canonical p53 REs is defined as 5'-Pu1-Pu2-Pu3-C4-A5/T5-3' and the complementary sequence 5'-A5/T5-G4-Py3-Py2-Py1-3'. From the crystal structures of p73 DBD bound to DNA that have been recently solved in our lab, we know that the p73 DBD makes both contacts to the bases and to the phosphate backbone of a canonical p53 RE (Figure 3.3). Residue Lys138 makes base specific contact with Pu2 on the top strand; Cys297 and Arg300 contact Py3 and G4 on the complementary strand. Residues Lys138, Ser261, Arg268, Arg293, and Ala296 contact the phosphate backbone of the DNA at position 1 on the top strand and positions 4 and 5 on the complementary

strand. G4 on the complementary strand shares two hydrogen bonds with Arg300, which highlighting the importance of this nucleotide.

The RE recognized by p73 shows certain degree of sequence degeneracy (Fontemaggi et al., 2002; Sbisa et al., 2007). Therefore, I would like to interpret the structure of p73 DBD and understand the essential DNA sequence requirements for p73 DBD to bind DNA. During the experiments, each nucleotide of the quarter-site was changed to a purine and a pyrimidine that are not commonly found in the consensus sequence. In addition, oligomeric states and binding affinities of p73 DBD with all the sequence variants were determined using analytical ultracentrifugation (AUC) and fluorescence anisotropy.

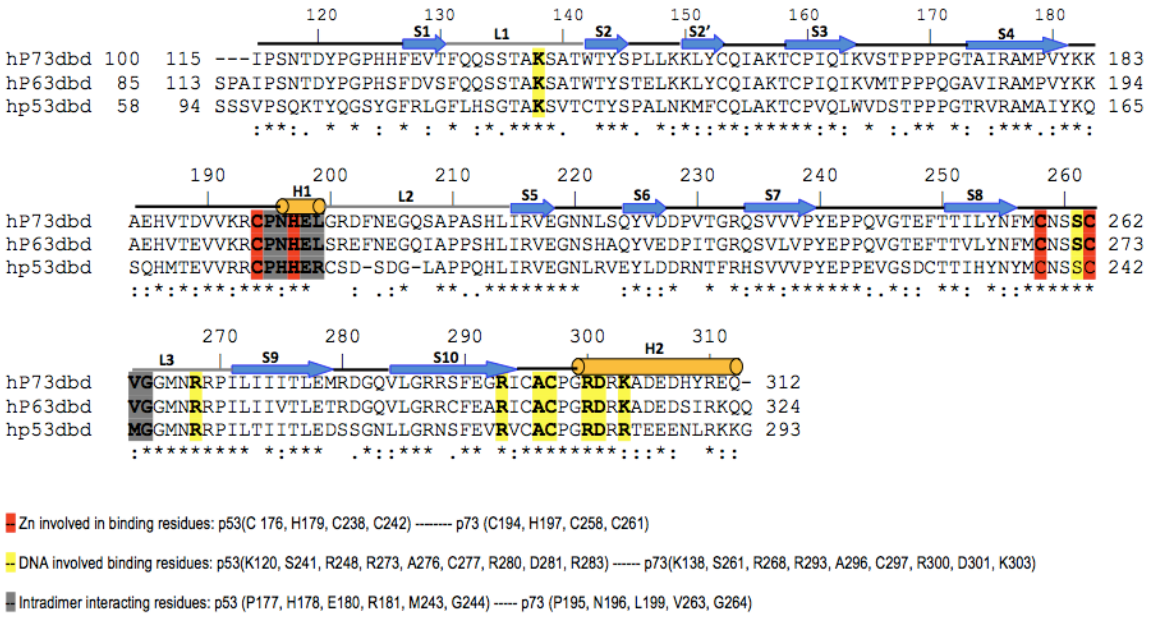

Figure 3.1. Sequence alignment of human DBDs of the p53 family proteins. The residues involved in DNA binding are highlighted in yellow, the Zn binding residues are highlighted in red, and the dimerization residues are highlighted in gray. The secondary structure of the p73 DBD is shown above the sequences. (Figure 3.1 courtesy of Dr. Abdul S. Ethayathulla.)

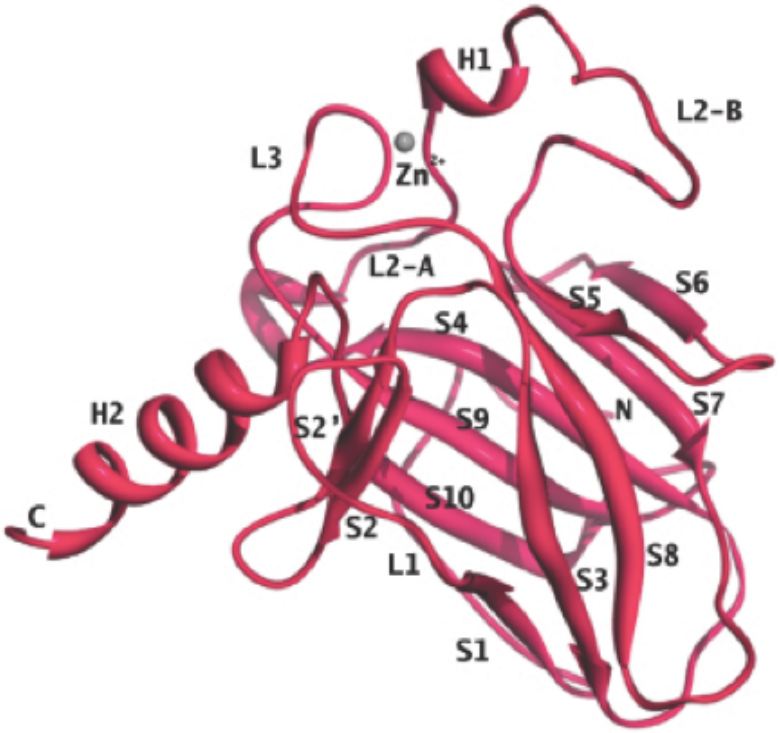

Figure 3.2. The X-ray crystal structure of p73 DBD. The structure of p73 DBD for forms an immunoglobulin-like β-sandwich fold, which consists of 11 β-strands (S1-S10), 2 helices (H1 and H2), and 3 loops (L1-L3). (Figure 3.2 courtesy of Dr. Abdul S. Ethayathulla.)

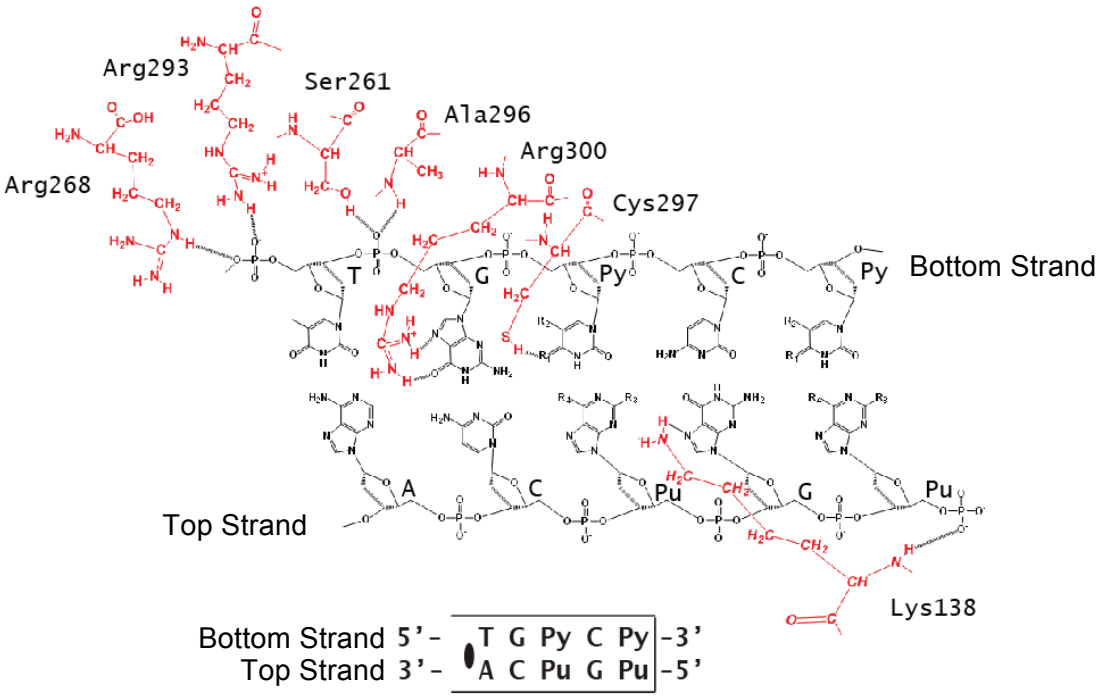

Figure 3.3. The interactions between p73 DBD and DNA. Residues involved in interactions with DNA sequences are shown as ligplot. (Figure 3.3 courtesy of Dr. Abdul S. Ethayathulla.)

B. Materials and Methods

1. Analytical ultracentrifugation (AUC)

Sedimentation velocity experiments were performed in 100 mM NaCl, 10 mM sodium citrate (pH 6.1), 5 mM DTT, and 5 μM $ZnCl_2$ using Beckman Optima XL-I analytical ultracentrifuge with a An-60 Ti rotor. For the protein experiment, 400 μL of buffer and 416 μM p73 DBD were loaded into a double-sector centerpiece. The experiment was carried out at 50,000 rpm, 20 °C, and the radial scans were collected at 280 nm. For the fluorescence experiments, 400 μL of buffer and protein-DNA complex containing 64.5 μM of p73 DBD and 3-3.4 μM of 5'-fluorescein-labeled dsDNA (Table 3.1) were loaded into double sector centerpieces. Experiments were carried out at 50,000 rpm, 20 °C, and the radial scans were collected at 488 nm. For the salt concentration experiments, 100 mM, 150 mM, 200 mM, 250 mM, 300 mM, and 400 mM NaCl were used. 400 μL of protein-DNA complexes containing 64.5 μM of p73 DBD and 3-3.4 μM of 5'-fluorescein-labeled dsDNA (12 bp, 5'-FAM/TGGGCATGCCCA-3'; 12 bp, 5'-FAM/ACCCGTACGGGT-3') at varying salt concentrations were loaded into the double sector centerpieces. Experiments were carried out at 50,000 rpm, 20 °C, and the radial scans were collected at 488 nm. Collected data were analyzed using SEDFIT software to calculate c(s) distributions (Lebowitz et al., 2002). SEDNTERP software was used to calculate the partial specific volume, buffer viscosity and buffer density (Laue et al., 1992).

2. Fluorescence Anisotropy

Fluorescence anisotropy experiments were performed in 100 mM NaCl, 10 mM sodium citrate (pH 6.1), 5 mM DTT, and 5 μM $ZnCl_2$. p73 DBD was serially diluted from 160 μM to 1 nM and there were a total of 17 tubes prepared with different concentrations at a final volume of 500 μL. The 5'-fluorescein-labeled dsDNA (Table 3.1) was added to each tube to a final concentration of 5 nM. The tubes were incubated on ice for 45 minutes, and the fluorescence intensity of each tube was measured using Hitachi F-2000 fluorescence spectrophotometer with excitation and emission wavelengths of 494 nm and 521 nm, respectively. The fluorescence anisotropy data was analyzed using non-linear regression curve with the Prism graphical software. 100 mM, 200 mM, and 300 mM NaCl were used in experiments for different salt concentrations with the 12 bp DNA 5'-FAM/TGGGCATGCCCA-3' and 5'-FAM/ACCCGTACGGGT-3'.

Table 3.1. Sequences of 12 bp fluorescein-labeled DNA. The sequences of fluorescein-labeled DNA that were used in the AUC and fluorescence anisotropy experiments.

	Sequence
12 bp	5′-FAM/TGGGCATGCCCA-3′ 3′-ACCCGTACGGGT/FAM-5′
12 bp	5′-FAM/TAGGCATGCCTA-3′ 3′-ATCCGTACGGAT/FAM-5′
12 bp	5′-FAM/TTGGCATGCCAA-3′ 3′-AACCGTACGGTT/FAM-5′
12 bp	5′-FAM/AGAGCATGCTCT-3′ 3′-TCTCGTACGAGA/FAM-5′
12 bp	5′-FAM/AGTGCATGCACT-3′ 3′-TCACGTACGTGA/FAM-5′
12 bp	5′-FAM/AGGACATGTCCT-3′ 3′-TCCTGTACAGGA/FAM-5′
12 bp	5′-FAM/AGGTCATGACCT-3′ 3′-TCCAGTACTGGA/FAM-5′
12 bp	5′-FAM/AGGGAATTCCCT-3′ 3′-TCCCTTAAGGGA/FAM-5′
12 bp	5′-FAM/AGGGGATCCCCT-3′ 3′-TCCCCTAGGGGA/FAM-5′
12 bp	5′-FAM/AGGGCGCGCCCT-3′ 3′-TCCCGCGCGGGA/FAM-5′
12 bp	5′-FAM/AGGGCTAGCCCT-3′ 3′-TCCCGATCGGGA/FAM-5′
12 bp	5′-FAM/ACCCGTACGGGT-3′ 3′-TGGGCATGCCCA/FAM-5′

C. Results

1. Determination of p73 DNA binding specificity at each nucleotide position within the consensus half-site.

In chapter 2, I have shown that p73 DBD has the highest binding affinity with 12 bp half-site than with smaller oligonucleotides. However, the question of how changes in the consensus sequence affect the DNA binding of the p73 DBD was not addressed. To further understand this relationship, I have changed the nucleotide at each position in the consensus half-site to a purine and a pyrimidine in order to determine the DNA binding specificity of the p73 DBD (Table 3.2). Figure 3.4 to Figure 3.9 show the sedimentation coefficient distribution of p73 DBD bound to different DNA sequences. When the nucleotide at position 1 was changed from guanine to either adenine or thymine, the sedimentation coefficients remained the same at 4.26 S (Figure 3.4). However, when the nucleotide at position 2 was changed from guanine to adenine, the sedimentation coefficient decreased from 4.29 S to 4.12 S, and it further decreased to 3.98 S when guanine changed to thymine (Figure 3.5). Moreover, when the nucleotide at position 3 was changed from guanine to adenine, the sedimentation coefficient was 4.36 S, while it decreased to 4.12 S when the nucleotide was changed to thymine (Figure 3.6). In addition, when the nucleotide at position 4 was changed from cytosine to adenine or guanine, the sedimentation coefficients were significantly lowered to 3.50 S and 3.38 S respectively (Figure 3.7). The sedimentation coefficient decreased to 3.94 S and 3.82 S when the nucleotide at position 5 was changed to guanine or thymine

(Figure 3.8). Lastly, when the nucleotides at all five positions were changed, the sedimentation coefficient decreased to 3.77 S (Figure 3.9).

Theoretically, the sedimentation coefficients for all p73 DBD complexes with 12 bp DNAs would be expected to be the same if their affinities would be identical. The differences in the AUC results might imply that p73 DBD has different binding affinities for the tested 12 bp DNA sequences. Therefore, I have carried out fluorescence anisotropy experiments to determine the p73 DBD binding affinities for those DNA sequences. The K_d for the 12 bp 5'-T**GGGCATG-CCC**A-3' was 2.83 μM. When the nucleotide at position 1 was changed to adenine, the K_d remained the same at 2.79 μM. Moreover, when the nucleotide was changed to thymine, the K_d increased to 11.62 μM (Figure 3.10). The effects of the nucleotides at position 2 and 3 were determined to be similar. When the nucleotides were changed from guanine to adenine at positions 2 and 3, the K_d slightly increased to 5.41 μM and 4.36 μM, respectively. The K_d increased even more to 7.82 μM and 9.94 μM when nucleotides were changed to thymine (Figure 3.11 and Figure 3.12). The K_d clearly increased to 23.48 μM and 32.89 μM when the nucleotide at position 4 was changed to adenine or guanine (Figure 3.13). This result showed the importance of cytosine at position 4. When the nucleotide at position 5 changed to guanine and thymine, the K_d increased to 11.77 μM and 14.17 μM (Figure 3.14). The binding affinity of p73 DBD weakened when nucleotide at position 5 was changed, but the effect was smaller compared to changes at position 4. When the nucleotides at all five positions were changed, the K_d increased to 19.32 μM (Figure 3.15).

2. The binding of p73 DBD to DNA is salt concentration dependent

The AUC and fluorescence anisotropy experiments were performed with 100 mM NaCl. To determine whether salt concentration would affect the DNA binding of p73 DBD, I performed experiments with 12 bp DNA with consensus DNA sequence 5'-T**GGGCATGCCC**A-3' and 12 bp DNA with non-consensus DNA sequence 5'-A**CCCGTACGGG**T-3' at various salt concentrations. I used 100, 150, 200, 250, 300, and 400 mM NaCl in the sedimentation velocity experiments. For the 12 bp consensus sequence, the sedimentation coefficient was 4.50 S with 100 mM NaCl. The sedimentation coefficients decreased when salt concentration increased. At the highest salt concentration of 400 mM NaCl, the sedimentation coefficient was 3.37 S (Figure 3.16). I also carried out fluorescence anisotropy experiments with 100, 200, and 300 mM NaCl. The K_d was determined to be 2.83 μM with 100 mM NaCl, and it increased when the salt concentration increased. The K_d values with 200 mM and 300 mM NaCl were 11.79 μM and 22.46 μM, respectively (Figure 3.17). For the non-consensus sequence, the effect on the salt concentration was similar to the consensus sequence. The sedimentation coefficient decreased and K_d increased as salt concentration increased. The sedimentation coefficient was 3.90 S with 100 mM NaCl, and it decreased to 2.84 S with 400 mM NaCl (Figure 3.18). The K_d was 19.32 μM for 100 mM NaCl, and it increased to 31.31 μM for 200 mM NaCl and 86.02 μM for 300 mM NaCl (Figure 3.19). These results indicated that the DNA binding of p73 DBD is salt concentration dependent. The salt concentration

experiment also confirmed that p73 DBD has a higher binding affinity towards a consensus DNA sequence than a non-consensus sequence.

Table 3.2. Sequences of 12 bp DNA. The sequences of 12 bp DNA that were used for the DNA binding specificity experiments. The quarter-sites are highlighted in blue, and the changed nucleotides are highlighted in red.

Sequence
1234554321
5′-TGGGCATGCCCA-3′ 3′-ACCCGTACGGGT-5′
5′-CAGGCATGCCTG-3′ 3′-GTCCGTACGGAC-5′
5′-ATGGCATGCCAT-3′ 3′-TACCGTACGGTA-5′
5′-AGAGCATGCTCT-3′ 3′-TCTCGTACGAGA-5′
5′-AGTGCATGCACT-3′ 3′-TCACGTACGTGA-5′
5′-AGGACATGTCCT-3′ 3′-TCCTGTACAGGA-5′
5′-AGGTCATGACCT-3′ 3′-TCCAGTACTGGA-5′
5′-AGGGAATTCCCT-3′ 3′-TCCCTTAAGGGA-5′
5′-AGGGGATCCCCT-3′ 3′-TCCCCTAGGGGA-5′
5′-AGGGCGCGCCCT-3′ 3′-TCCCGCGCGGGA-5′
5′-AGGGCTAGCCCT-3′ 3′-TCCCGATCGGGA-5′
5′-ACCCGTACGGGT-3′ 3′-TGGGCATGCCCA-5′

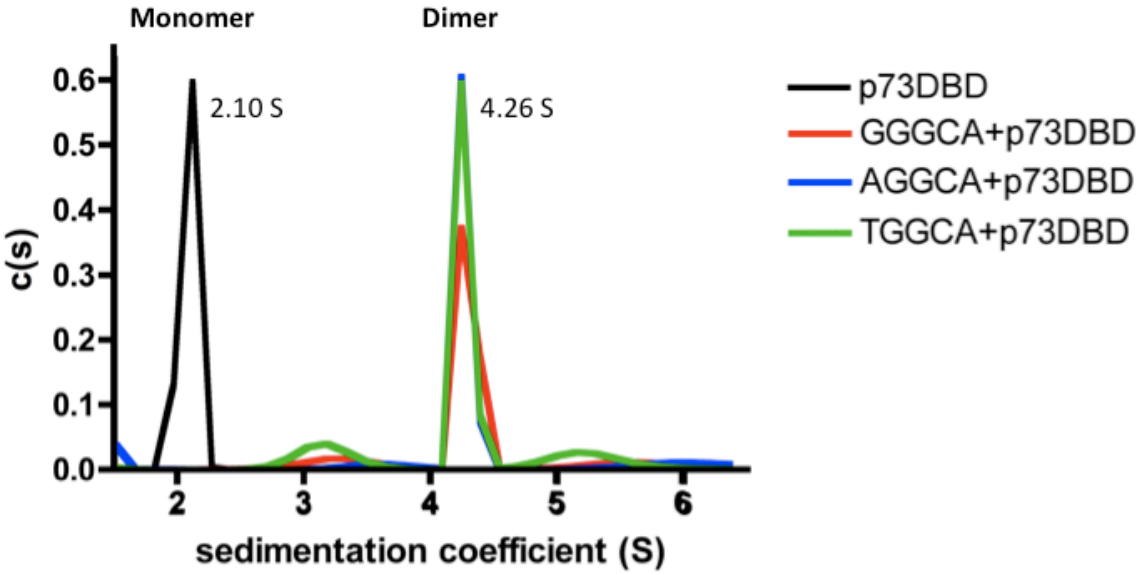

Figure 3.4. Sedimentation coefficient distribution of 8His-p73 DBD with nucleotide changed at the first position of 12 bp DNA.

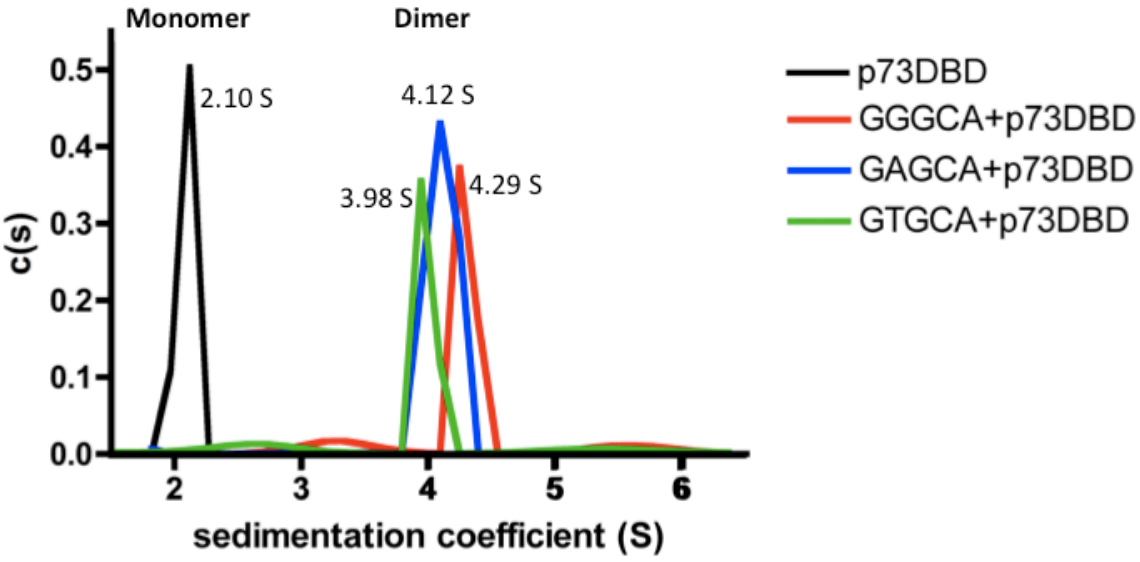

Figure 3.5. Sedimentation coefficient distribution of 8His-p73 DBD with nucleotides changed at the second position of 12 bp DNA.

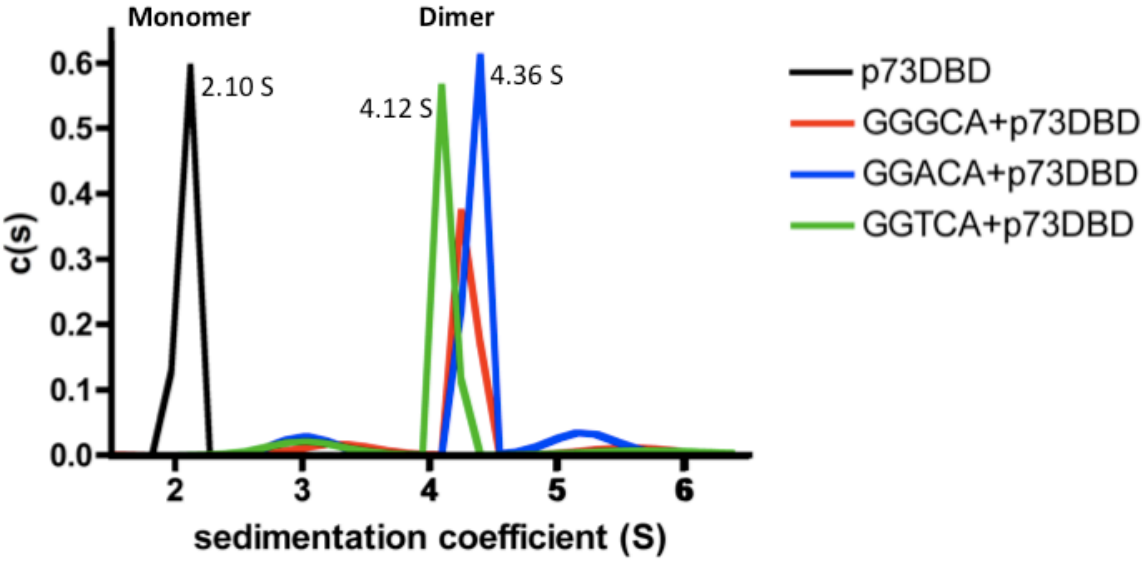

Figure 3.6. Sedimentation coefficient distribution of 8His-p73 DBD with nucleotides changed at the third position of 12 bp DNA.

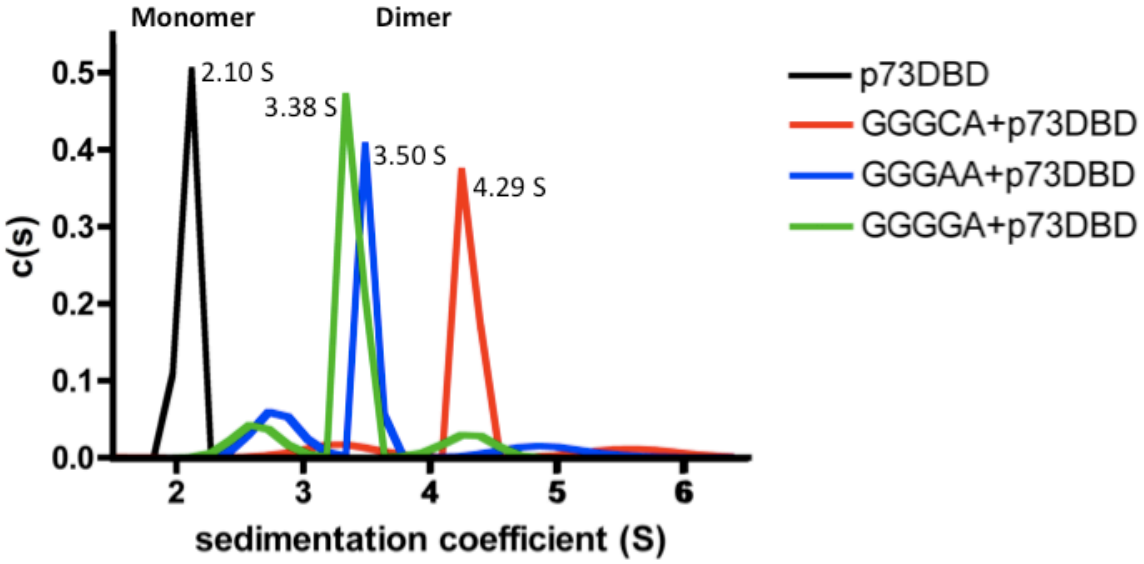

Figure 3.7. Sedimentation coefficient distribution of 8His-p73 DBD with nucleotides changed at the fourth position of 12 bp DNA.

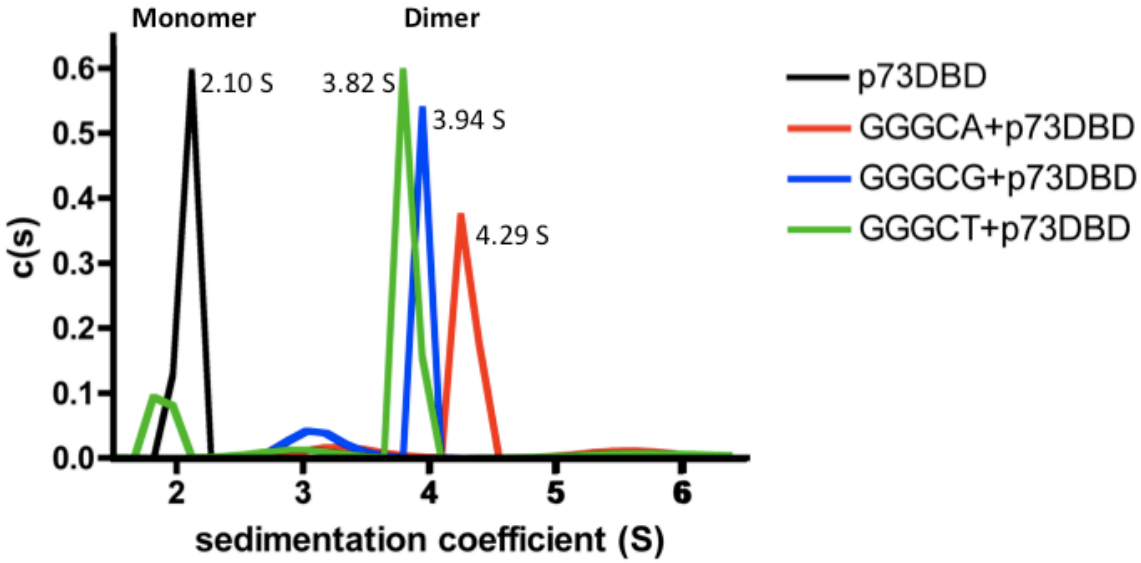

Figure 3.8. Sedimentation coefficient distribution of 8His-p73 DBD with nucleotides changed at the fifth position of 12 bp DNA.

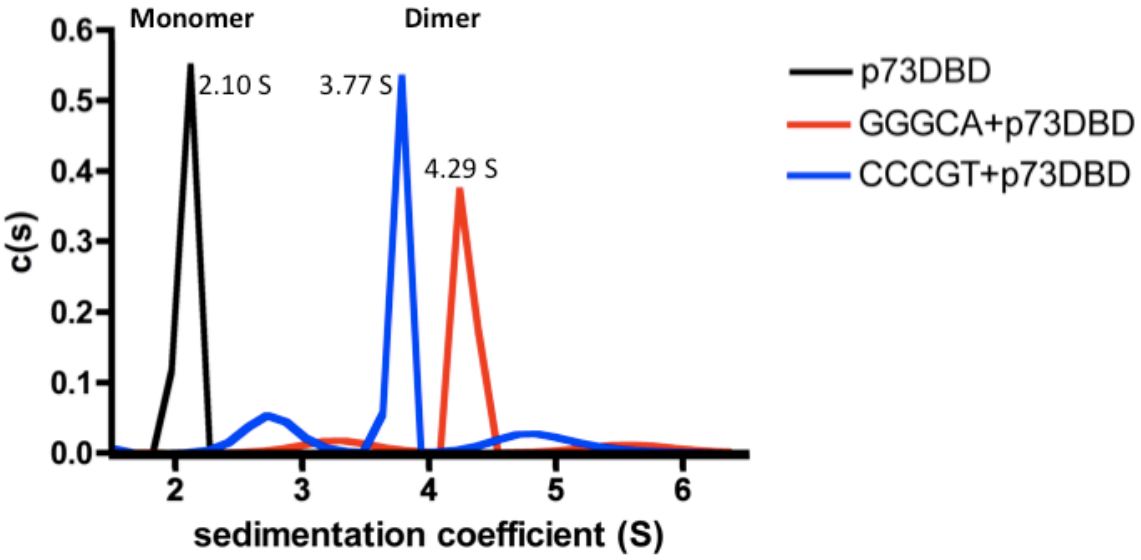

Figure 3.9. Sedimentation coefficient distribution of 8His-p73 DBD with nucleotides changed at all five positions of 12 bp DNA.

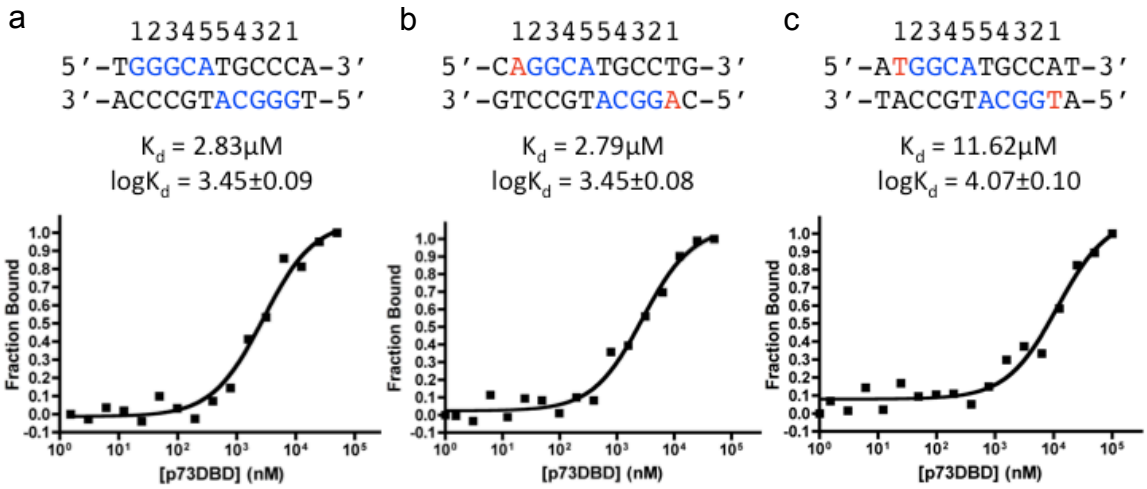

Figure 3.10. Fluorescence Anisotropy of 8His-p73 DBD with nucleotide changed at the first position of 12 bp DNA. The dissociation constant (K_d) of p73 DBD with a) GGGCA quarter-site is 2.825 μM; b) AGGCA quarter-site is 3.445 μM; and c) TGGCA quarter-site is 11.623 μM.

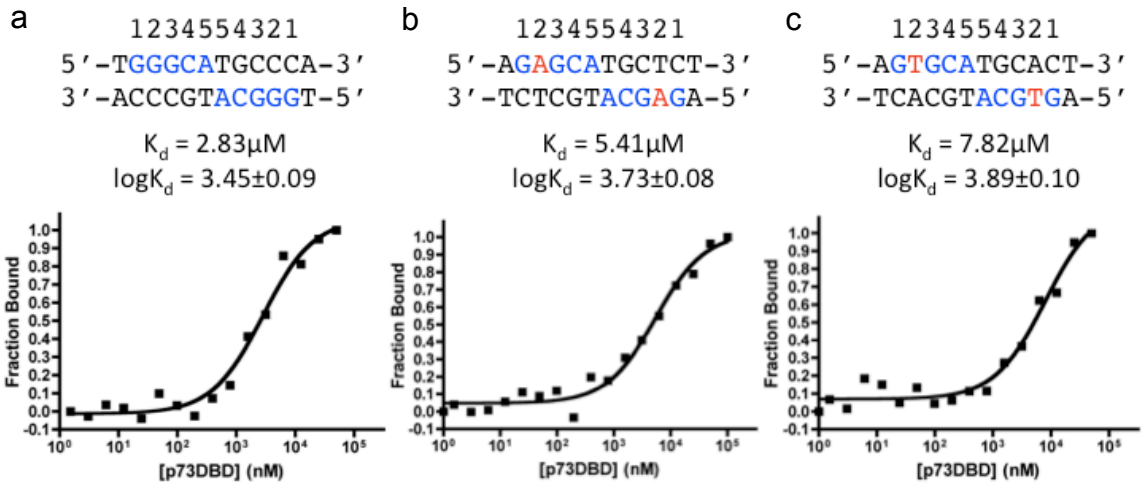

Figure 3.11. Fluorescence Anisotropy of 8His-p73 DBD with nucleotide changed at the second position of 12 bp DNA. The dissociation constant (K_d) of p73 DBD with a) GGGCA quarter-site is 2.825 μM; b) GAGCA quarter-site is 5.406 μM; and c) GTGCA quarter-site is 7.815 μM.

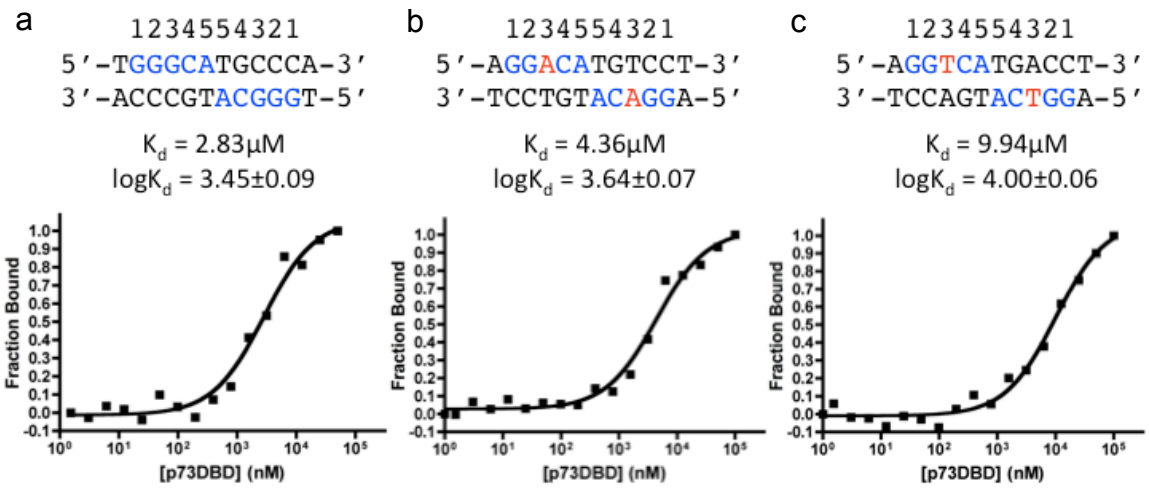

Figure 3.12. Fluorescence Anisotropy of 8His-p73 DBD with nucleotide changed at the third position of 12 bp DNA. The dissociation constant (K_d) of p73 DBD with a) GGGCA quarter-site is 2.825 μM; b) GGACA quarter-site is 4.360 μM; and c) GGTCA quarter-site is 9.942 μM.

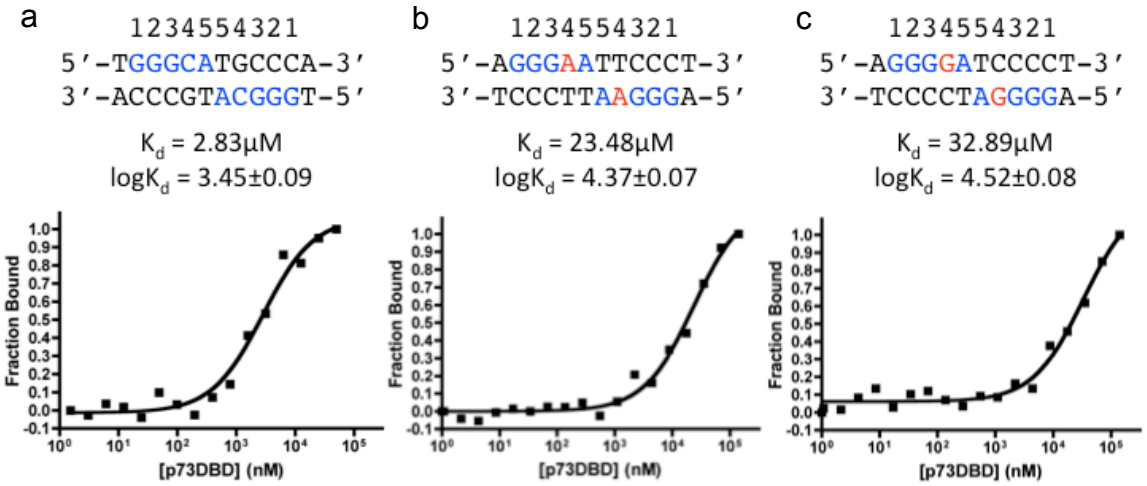

Figure 3.13. Fluorescence Anisotropy of 8His-p73 DBD with nucleotide changed at the fourth position of 12 bp DNA. The dissociation constant (K_d) of p73 DBD with a) GGGCA quarter-site is 2.825 μM; b) GGGAA quarter-site is 23.48 μM; and c) GGGGA quarter-site is 32.89 μM.

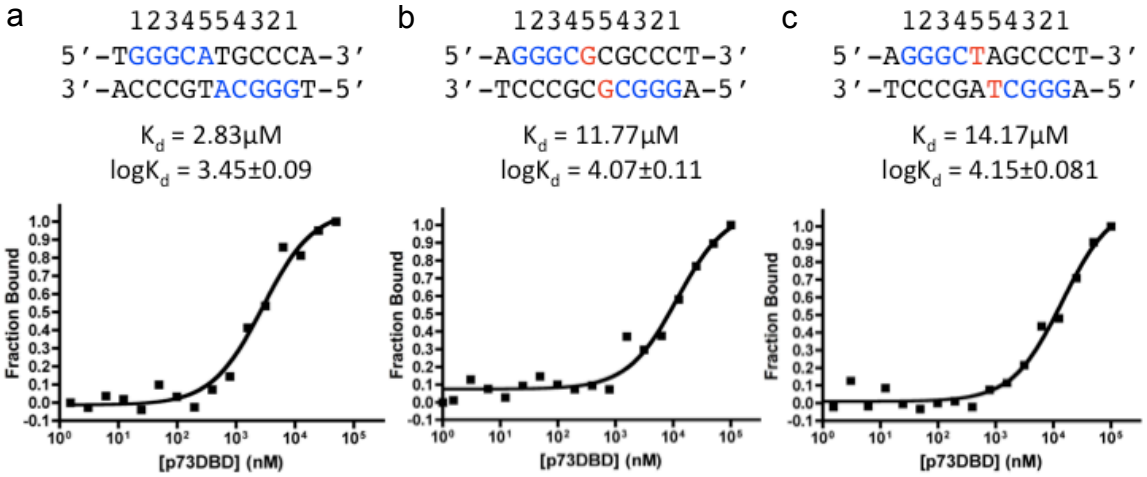

Figure 3.14. Fluorescence Anisotropy of 8His-p73 DBD with nucleotide changed at the fifth position of 12 bp DNA. The dissociation constant (K_d) of p73 DBD with a) GGGCA quarter-site is 2.825 μM; b) GGGCG quarter-site is 11.77 μM; and c) GGGCA quarter-site is 14.17 μM.

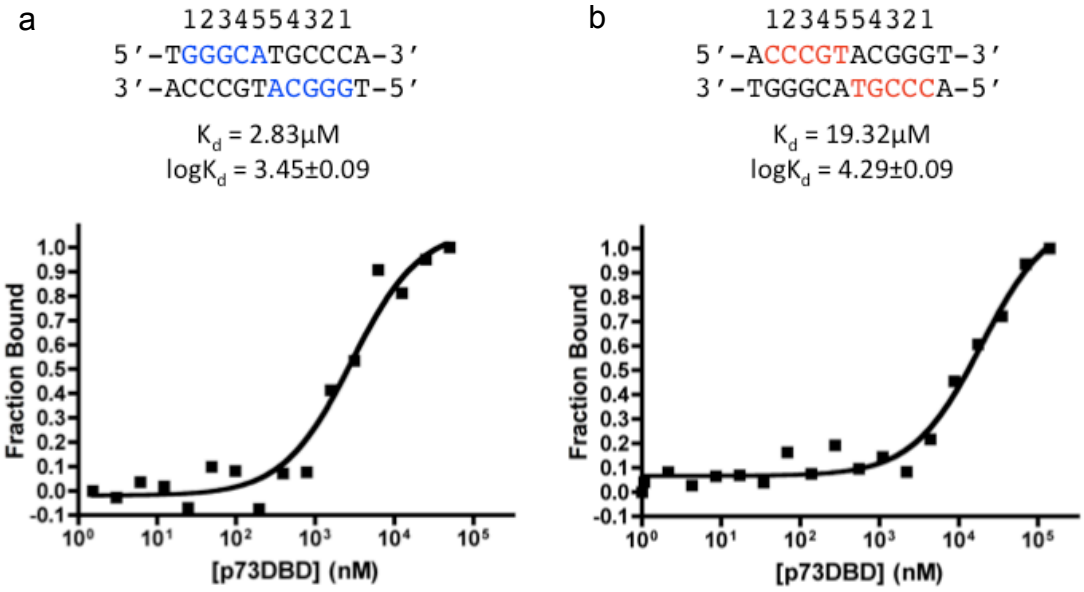

Figure 3.15. Fluorescence Anisotropy of 8His-p73 DBD with nucleotide changed at all five positions of 12 bp DNA. The dissociation constant (K_d) of p73 DBD with a) GGGCA quarter-site is 2.825 μM; and b) CCCGT quarter-site is 19.32 μM.

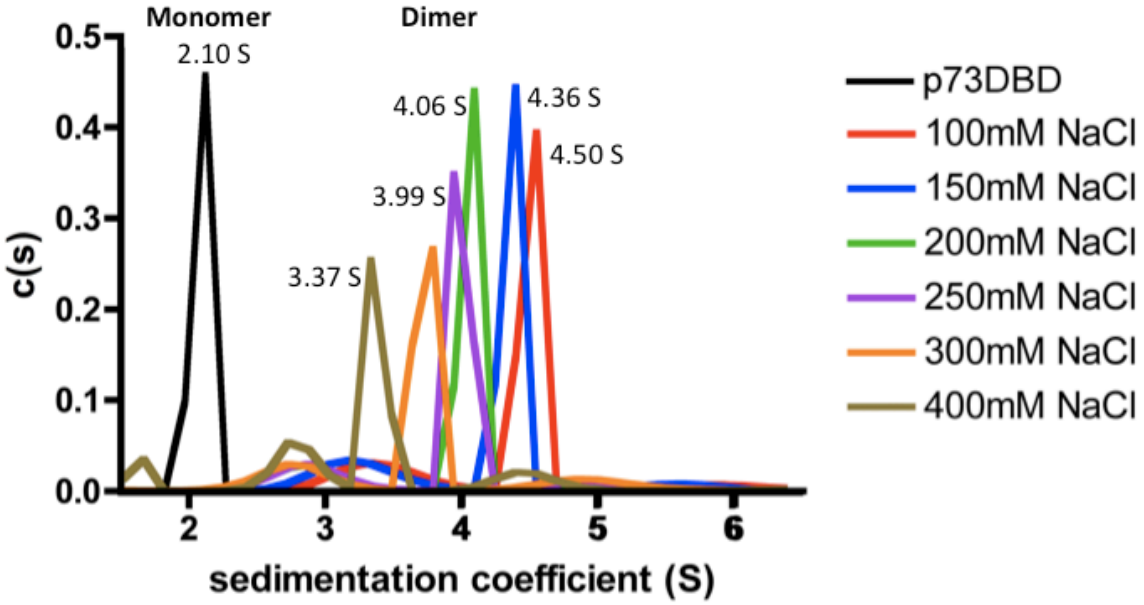

Figure 3.16. Sedimentation coefficient distribution of 8His-p73 DBD with 12 bp DNA with quarter-site of GGGCA at different salt concentrations.

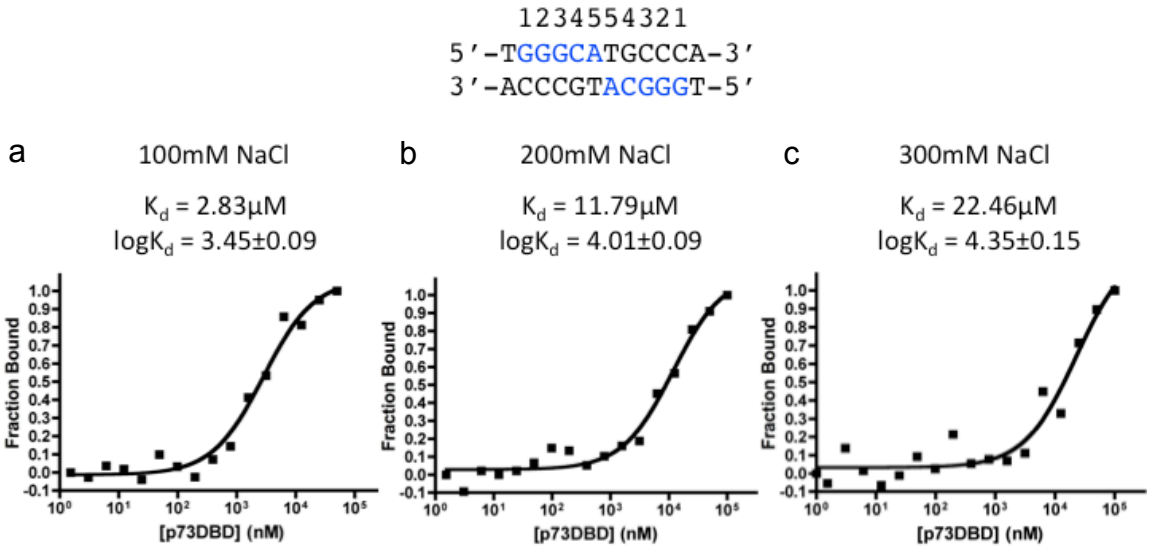

Figure 3.17. Fluorescence Anisotropy of 8His-p73 DBD with 12 bp DNA with quarter-site of GGGCA at different salt concentrations. The dissociation constant (K_d) of p73 DBD with a) 100 mM NaCl is 2.825 µM; b) 200 mM NaCl is 11.79 µM; and c) 300 mM NaCl is 22.46 µM.

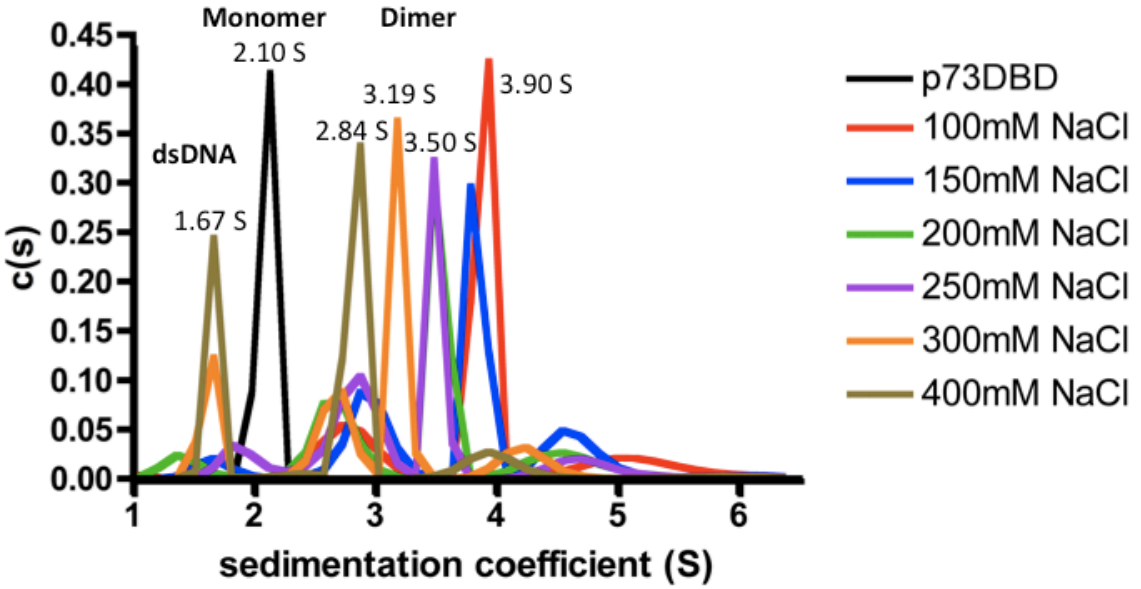

Figure 3.18. Sedimentation coefficient distribution of 8His-p73 DBD with 12 bp DNA with quarter-site of CCCGT at different salt concentrations.

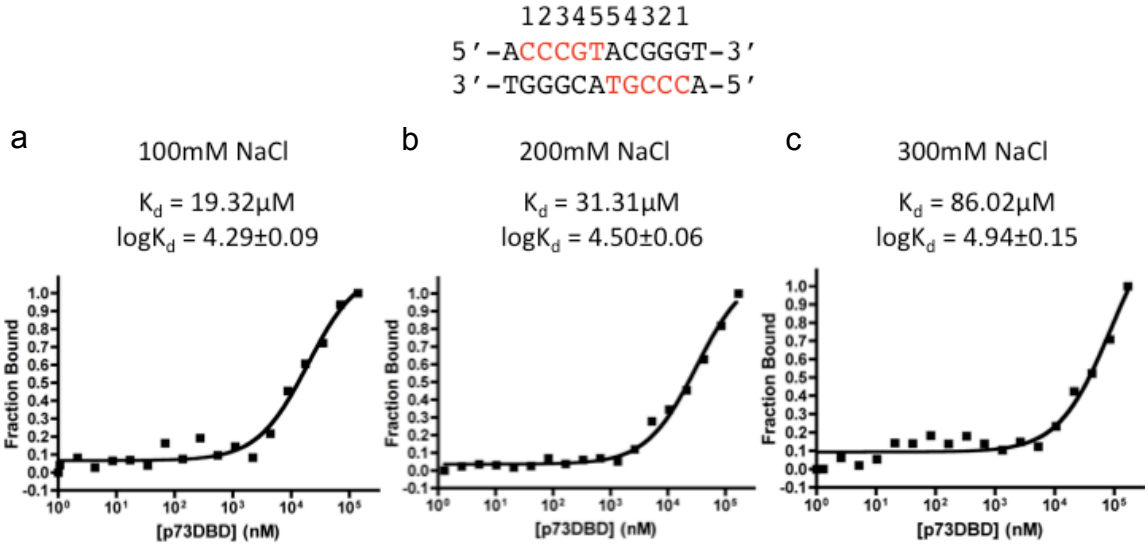

Figure 3.19. Fluorescence Anisotropy of 8His-p73 DBD with 12 bp DNA with quarter-site of CCCGT at different salt concentrations. The dissociation constant (K_d) of p73 DBD with a) 100 mM NaCl is 19.32 μM; b) 200 mM NaCl is 31.31 μM; and c) 300 mM NaCl is 86.02 μM.

D. Discussion

In sedimentation velocity experiments, molecules sediment separately based on their size and shape. The larger the molecule is, the faster it sediments to the bottom of the AUC cell. p73 DBD binds to various DNA sequences with different affinities, hence different protein-DNA dissociation rates are observed. A higher dissociation rate implies a weaker binding affinity and a lower sedimentation coefficient (S-value), because longer time is needed for the complex to sediment. In contrary, the p73 DBD:DNA complex would have a larger sedimentation coefficient if it has a stronger DNA binding affinity (smaller K_d). From the experimental results, the sedimentation coefficients determined by AUC are well correlated with the K_d determined by fluorescence anisotropy; i.e. the S-value is inversely proportional to the K_d (Table 3.3 and Figure 3.20). p73 DBD binds to consensus DNA with similar affinity. When the consensus purines at positions 1, 2, and 3 were changed from G to A, the K_d remained similar; however, when these consensus purines were changed from G to T, which is a pyrimidine, the K_d values significantly increased. Changing the consensus sequence at positions 4 and 5 also decreased the p73 DNA binding affinity. Among all the changes at every position, the changes at position 4 made the most dramatic decrease in the binding affinity (K_d increased 7-10 fold from ~3 μM to ~30 μM) (Table 3.3). From the crystal structure of p73 DBD bound to DNA, it is known that G at position 4 (complementary strand of DNA) makes two hydrogen bonds with Arg300 of p73. As expected from the structural data, changes at

position 4 of the consensus sequence abolish the hydrogen bonds, therefore decrease the p73 DBD binding affinity dramatically.

The non-consensus DNA with changes at all five positions is defective in binding. However, it is surprised that this particular non-consensus DNA with sequence CCCGT showed higher binding affinity than the single nucleotide change at position 4 (K_d = 19.32 μM vs. 32.89 μM) (Figure 3.13, 3.15, and Table 3.3). One possible explanation of this observation is that p73 might slightly slide on DNA back and forth when it encounters different DNA sequences, and it recognizes the C at position 3 (CCCGT) in this particular case as the C is as position 4 in the original consensus site. Therefore, the hydrogen bonding made by the complementary G is partially maintained. In order to further study this question, we should use various non-consensus DNA sequences.

From the salt concentration experiment, p73 DNA binding affinity is salt concentration dependent. The higher the salt concentration is, the weaker the DNA binding becomes (Figure 3.16 and 3.18). Moreover, the salt concentration experiment further confirms that p73 DBD has a higher binding affinity towards a consensus DNA sequence than a non-consensus sequence. The K_d of the consensus DNA, 5'-TGGGCATGCCCA-3', is always smaller than the K_d of the non-consensus DNA, 5'-ACCCGTACGGGT-3', at various salt concentrations (Figure 3.17 and 3.19).

Table 3.3. Table of sedimentation coefficient (S-value) vs. K_d. Sequences were shown with quarter-site, and the changed nucleotides were highlighted in red.

	DNA sequence 12345	S-value	K_d (μM)
Consensus	12b.p.-GGGCA	4.29	2.83
	12b.p.-AGGCA	4.26	2.79
	12b.p.-GAGCA	4.12	5.41
	12b.p.-GGACA	4.36	4.36
Change at position 1	12b.p.-TGGCA	4.26	11.62
Change at position 2	12b.p.-GTGCA	3.98	7.82
Change at position 3	12b.p.-GGTCA	4.12	9.94
Change at position 5	12b.p.-GGGCG	3.94	11.77
	12b.p.-GGGCT	3.82	14.17
Change at position 4	12b.p.-GGGAA	3.50	23.48
	12b.p.-GGGGA	3.38	32.89
Change at all positions	12b.p.-CCCGT	3.77	19.32

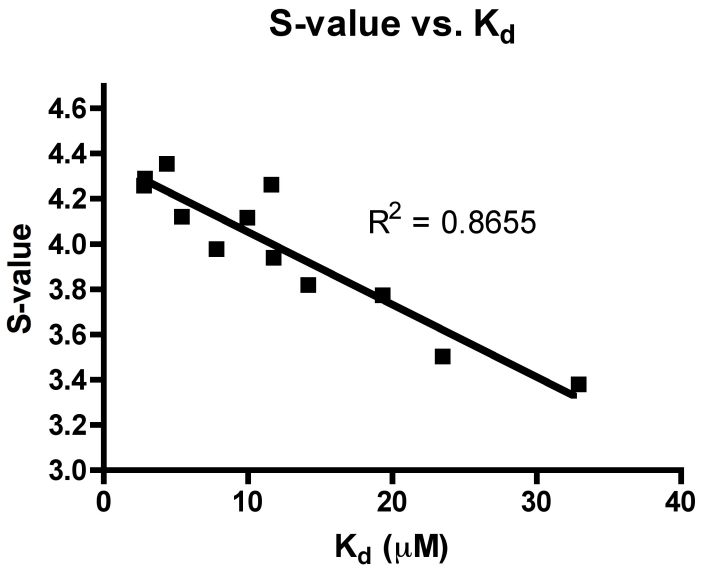

Figure 3.20. The graph of sedimentation coefficient (S-value) vs. K_d. Trendline and R^2 are indicated.

E. References

Chen, C., Gorlatova, N., Kelman, Z., and Herzberg, O. (2011). Structures of p63 DNA binding domain in complexes with half-site and with spacer-containing full response elements. Proc Natl Acad Sci U S A *108*, 6456-6461.

Cho, Y., Gorina, S., Jeffrey, P.D., and Pavletich, N.P. (1994). Crystal structure of a p53 tumor suppressor-DNA complex: understanding tumorigenic mutations. Science *265*, 346-355.

Fontemaggi, G., Kela, I., Amariglio, N., Rechavi, G., Krishnamurthy, J., Strano, S., Sacchi, A., Givol, D., and Blandino, G. (2002). Identification of direct p73 target genes combining DNA microarray and chromatin immunoprecipitation analyses. J Biol Chem *277*, 43359-43368.

Laue, T.M., Shah, B.D., Ridgeway, T.M., and Pelletier, S.L. (1992). Computer-Aided Interpreation of Analytical Sedimentation Data for Proteins. In Analytical Ultracentrifugation in Biochemistry and Polymer Science, S.E. Harding, A.J. Rowe, and J.C. Horton, eds. (Royal Society of Chemistry).

Lebowitz, J., Lewis, M.S., and Schuck, P. (2002). Modern analytical ultracentrifugation in protein science: a tutorial review. Protein science : a publication of the Protein Society *11*, 2067-2079.

Sbisa, E., Catalano, D., Grillo, G., Licciulli, F., Turi, A., Liuni, S., Pesole, G., De Grassi, A., Caratozzolo, M.F., D'Erchia, A.M.*, et al.* (2007). p53FamTaG: a database resource of human p53, p63 and p73 direct target genes combining in silico prediction and microarray data. BMC Bioinformatics *8 Suppl 1*, S20.

Chapter 4

Expression and Purification of p73 Isoforms

A. Introduction

In cells, p73 exists as various isoforms generated by alternative splicing and alternative promoter usage. The human *TP73* gene encodes 29 different isoforms. There are two different promoters in the *TP73* gene, the TA promoter and the ΔN promoter, which generate two major isoforms: TAp73 with a full N-terminal transactivation domain (TAD) and the N-terminal truncated p73 (ΔNp73) that lacks the TAD and it is therefore transcriptional inactive (Figure 1.3) (Yang et al., 2000). Alternative splicing at the C-terminal end of the *TP73* gene generates seven major isoforms, α, β, γ, δ, ε, ζ, and η, which have different regulatory and transcriptional activities (De Laurenzi et al., 1998; De Laurenzi et al., 1999; Kaghad et al., 1997).

As described in the introduction, full-length p73 is formed by a N-terminal transactivation domain (TAD), a DNA-binding domain (DBD), a tetramerization domain (TD) and C-terminal sterile alpha motif domain (SAM) and inhibitory domain (ID). In previous chapters, I have studied the DNA binding properties of p73 DBD. In this chapter, I would like to further investigate the DNA binding properties using the full-length protein of diverse p73 isoforms. Among all this isoforms, I have chosen to study four of them: TAp73α, ΔNp73α, TAp73δ, and ΔNp73δ (Figure 4.1). The TAp73α isoform is the wild type (wt) full-length protein, which has both the complete N-terminal TAD and complete C-terminal SAM and ID. The δ isoforms lack the C-terminal SAM and ID and have been shown to reduce transcriptional activity (Ueda et al., 2001); the ΔNp73 isoforms lack the N-terminal TAD which functions as a dominant-negative transcriptional inhibitor of

TAp73 by forming inactive heterotetramer and by competing for target DNA binding sites (Yang et al., 2000).

Figure 4.1. Domain Organization of TAp73α, ΔNp73α, TAp73δ, and ΔNp73δ. The full-length p73 consists of Transactivation domain (TAD), Proline Rich Region (PRR), DNA-binding domain (DBD), tetramerization domain (TD), and C-terminal Sterile Alpha Motif (SAM) domain and inhibitory domain (ID). The lines in red indicates the regions that are different from the full-length p73.

B. Materials and Methods

1. Cloning

The DNA fragment encoding human p73 isoforms (TAp73α: amino acid residues 1-636; ΔNp73α: amino acid residues 1-587; TAp73δ: amino acid residues 1-403; and ΔNp73δ: amino acid residues 1-354) was amplified by PCR using a template of human 8His-TAp73α (1-636). The forward primer containing EcoRI restriction site 5'-GAGAGAATTCATGCTGTATGTCGGTGACCCAGCCC-GCCACCTGGCAACCGCACAATTCAACCTGTTA-3' and the reverse primer containing HindIII restriction site 5'-TGGTAAGCTTAGTGGATTTCTGCTTCGGT-3' were used for ΔNp73α. The forward primer containing EcoRI restriction site 5'-GAGAGAATTCATGGCCCAAAGCACCGCG-3' and the reverse primer containing HindIII restriction site 5'-TGGTAAGCTTATGGACCCCAGGTTGGAC-GCTGCAGTAATTG-3' were used for TAp73δ. The forward primer containing EcoRI restriction site 5'-GAGAGAATTCATGCTGTATGTCGGTGACCCAGCCC-GCCACCTGGCAACCGCACAATTCAACCTGTTA-3' and the reverse primer containing HindIII restriction site 5'-TGGTAAGCTTATGGACCCCAGGTTGGAC-GCTGCAGTAATTG-3' were used for ΔNp73δ. The PCR product was cloned into the pET28a vector (Novagen).

2. Proteins Expression and Purification

The recombinant plasmids of p73 isoforms were transformed into *E. coli* BL21/DE3 cells. The cells were expressed in LB medium containing 30 μg/mL kanamycin at 37 °C until OD_{600nm} reached 0.6-0.8, and the cells were induced

with 0.5 mM isopropyl-β-D-thiogalactopyranoside (IPTG) at 25 °C for 5 hours. The cells were harvested by centrifugation and resuspended in a buffer containing 500 mM NaCl, 50 mM Tris-HCl (pH 8.0), 20 mM imidazole. The cells were then lysed by french press with addition of 1 mM phenylmethanesulfonylfluoride protease inhibitor (PMSF). The cell lysate was centrifuged by ultracentrifugation at 30,000 rpm, 4 °C for 30 minutes. The soluble fraction was incubated with 2 mL of Ni-NTA resin (QIAGEN) at 4°C for 1 hour and transferred into a gravity column. For the TAp73α construct, the resin was washed with 100 mL of the lysis buffer. The protein was first eluted with 80mM imidazole and collected in 1 mL fractions, and then was eluted with increasing imidazole concentrations (100 – 300 mM) and collected in 3mL fractions. For the ΔNp73α, TAp73δ, and ΔNp73δ constructs, the resin was washed with 100 mL of the lysis buffer. The proteins were eluted with increasing imidazole concentrations (100 mM – 1 M) and 3 mL fractions were collected. The proteins purified from the affinity column were analyzed by SDS-PAGE (10 %, w/v) followed by Coomassie staining and western blotting using anti-His antibody (Roche, 0490527001). For each p73 isoform, the protein was further purified by gel filtration chromatography using Superdex 200 column. The column was equilibrated using a buffer with 500 mM NaCl, 50 mM Tris-HCl (pH 8.0), 20 mM imidazole. The samples of p73 isoforms were loaded onto the column at room temperature at a flow rate of 0.5 mL/min. Absorbance was recorded at 280 nm. Purified proteins were analyzed by SDS-PAGE (10 %, w/v) followed by

Coomassie staining and western blotting using anti-His antibody (Roche, 0490527001).

C. Results

1. Recombinant α isoforms form tetramers in solution.

To investigate the oligomerization state of full-length p73 (TAp73α isoform), the recombinant human 8His-TAp73α was expressed in *E. coli* and purified from Ni affinity chromatography (Figure 4.2), followed by gel filtration chromatography (Figure 4.3). The superdex-200 gel filtration chromatography elution profile shows four peaks, P1 - P4 (Figure 4.3a). P1 was eluted in the column void volume, which indicates the protein was aggregated. Comparing the other peaks with the molecular weight standards indicates P2, eluting with a MW of 324 kDa, is the tetramerization state of the protein; P3, with a MW of 75 kDa, is the monomeric state of the protein; and P4, with a MW of 28 kDa, might be the degradation products of the protein or other impurities. This elution profile suggests that TAp73α assembled into tetramers in solution by gel filtration chromatography.

Similarly, the recombinant human 8His-ΔNp73α was expressed in *E. coli* and purified using the same purification scheme as 8His-TAp73α (Figure 4.4 and 4.5). The majority of 8His-ΔNp73α was eluted as tetramers (P2) in gel filtration chromatography.

2. Recombinant δ isoforms form large molecular weight oligomers in solution.

The recombinant human 8His-TAp73δ was also expressed and purified from *E. coli* using the same purification scheme as 8His-TAp73α (Figure 4.6 and

4.7). However, the majority of the protein was eluted as large MW oligomers (P2) in gel filtration chromatography, with an approximate MW of 361 kDa.

The recombinant human 8His-ΔNp73δ was expressed and purified from *E. coli* using Ni affinity chromatography. The protein purification results showed significant amount of impurities in the elution from Ni affinity chromatography (Figure 4.8).

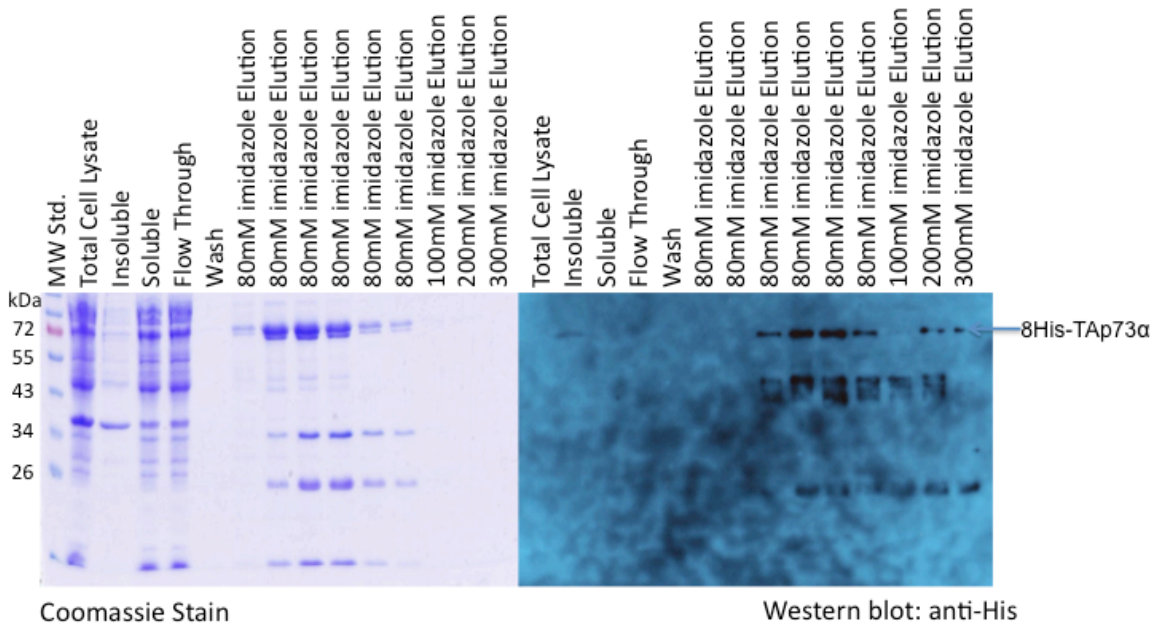

Figure 4.2. Purification of recombinant human 8His-TAp73α (1-636) using Ni affinity chromatography. Coomassie stain (left) and western blot (right) of 10 % SDS-PAGE analysis showed TAp73α migrated at ~72 kDa.

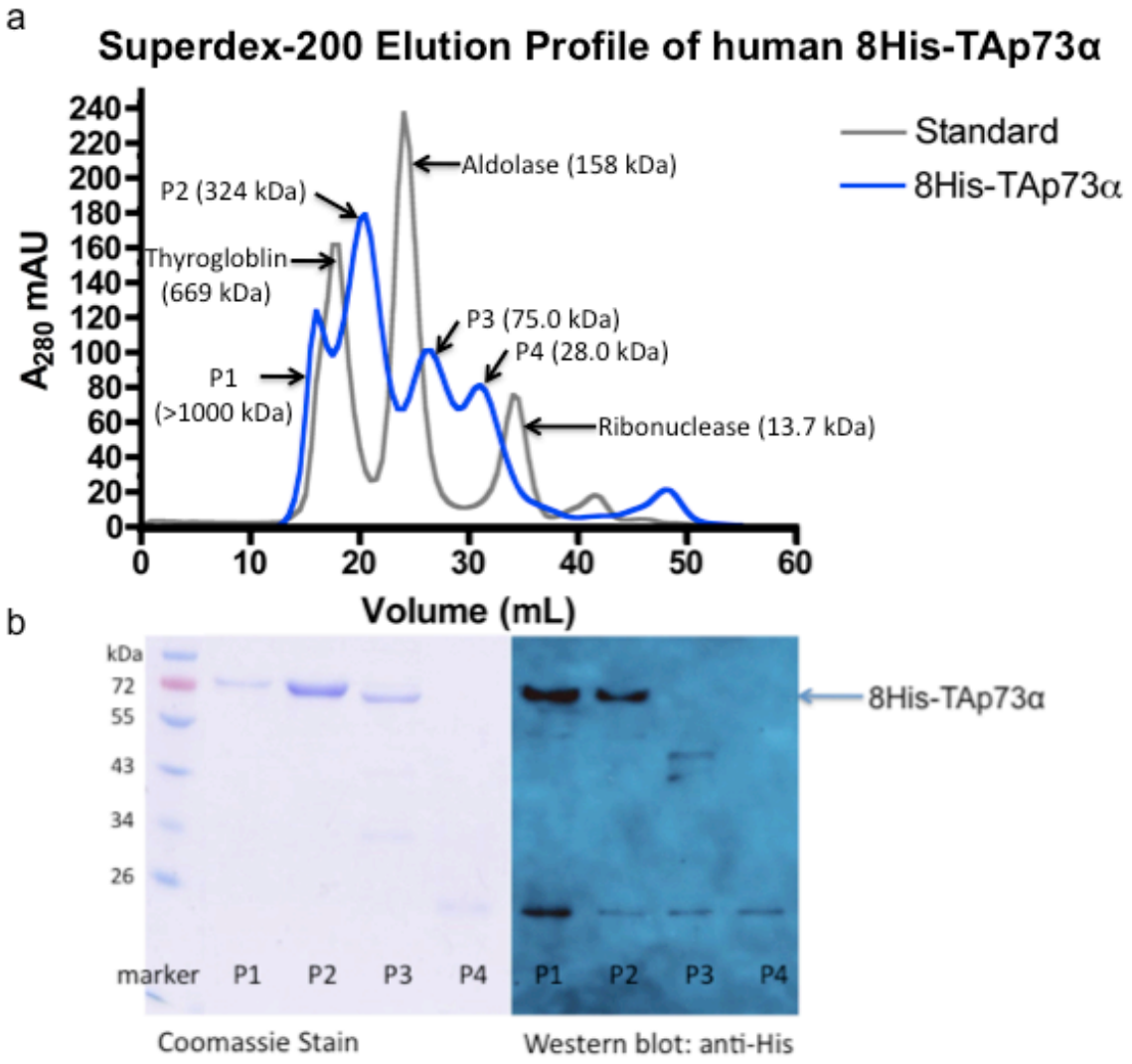

Figure 4.3. Purification of recombinant human 8His-TAp73α (1-636) using gel filtration chromatography. a) Superdex-200 gel filtration chromatography elution profile. Overlaying with MW standard indicates 8His-TAp73α forms tetramer in solution (P2). b) 10 % SDS-PAGE analysis of superdex-200 elutions.

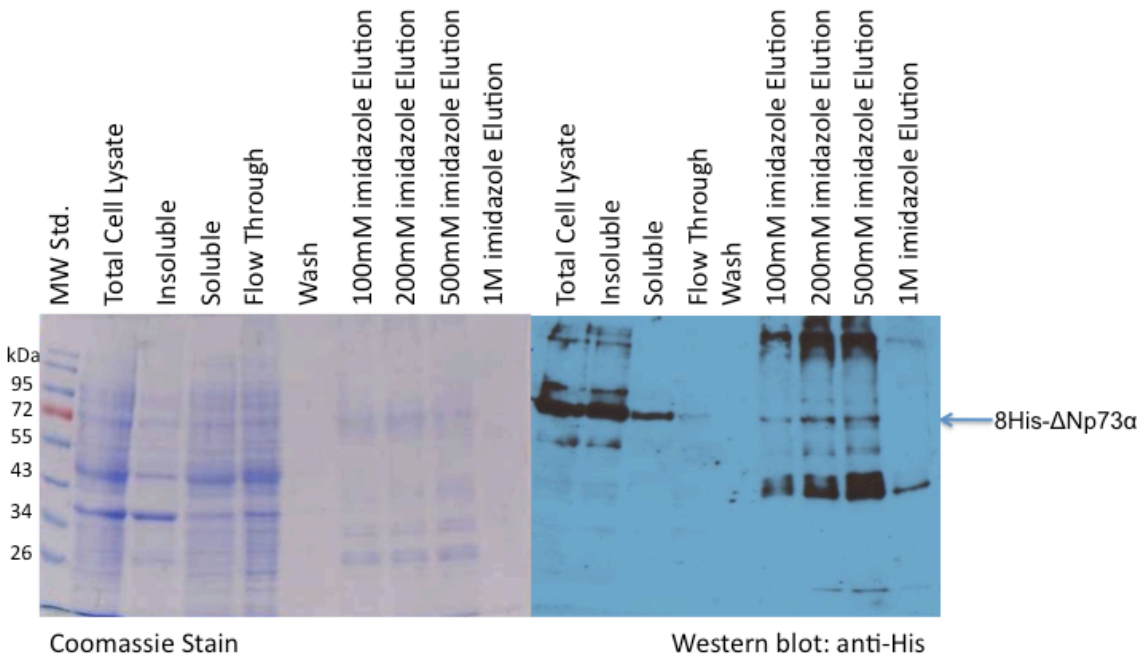

Figure 4.4. Purification of recombinant human 8His-ΔNp73α (1-587) using Ni affinity chromatography. Coomassie stain (left) and western blot (right) of 10 % SDS-PAGE analysis showed TAp73α migrated at ~72 kDa.

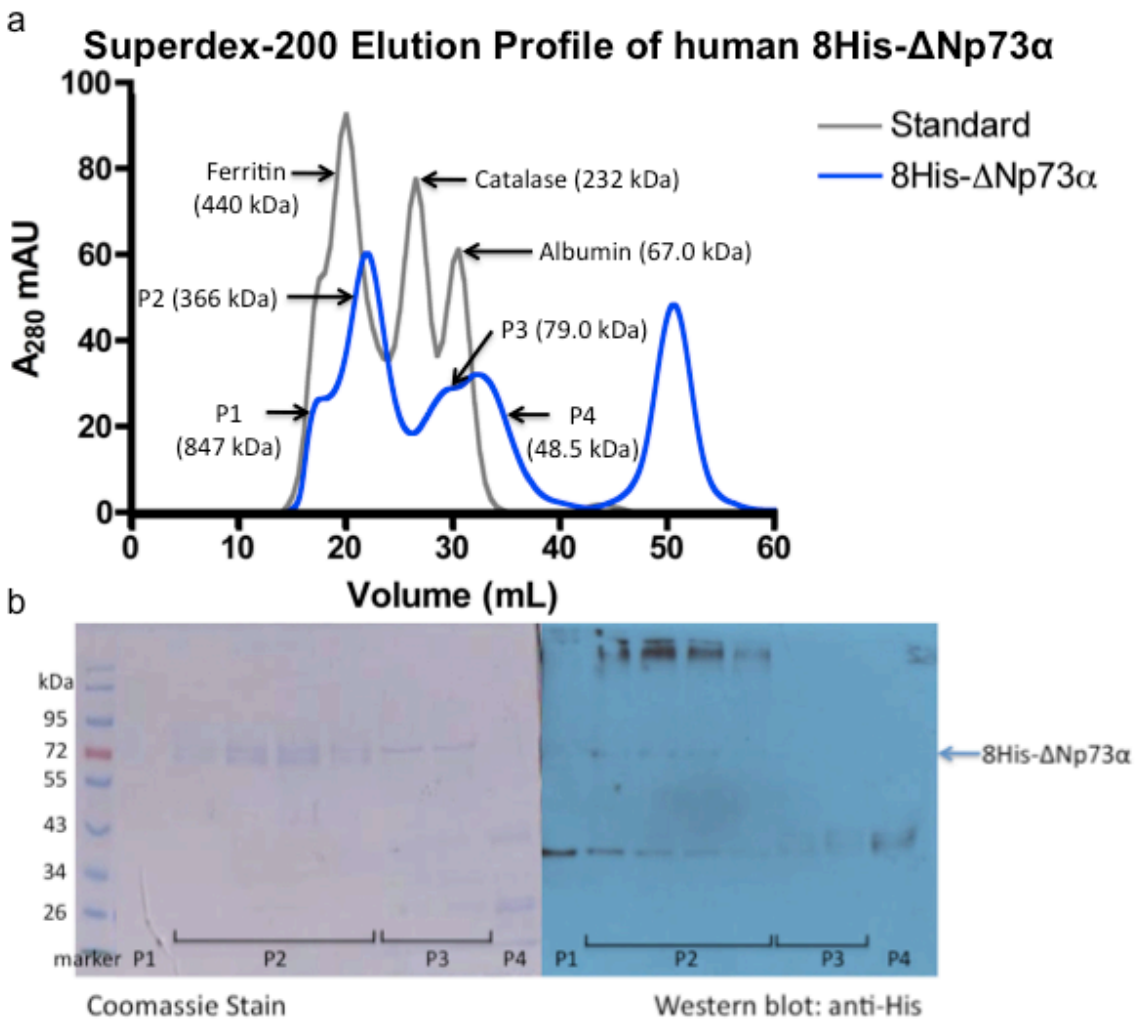

Figure 4.5. Purification of recombinant human 8His-ΔNp73α (1-587) using gel filtration chromatography. a) Superdex-200 gel filtration chromatography elution profile. Overlaying with MW standard indicates 8His-ΔNp73α forms tetramer in solution (P2). b) 10 % SDS-PAGE analysis of superdex-200 elutions.

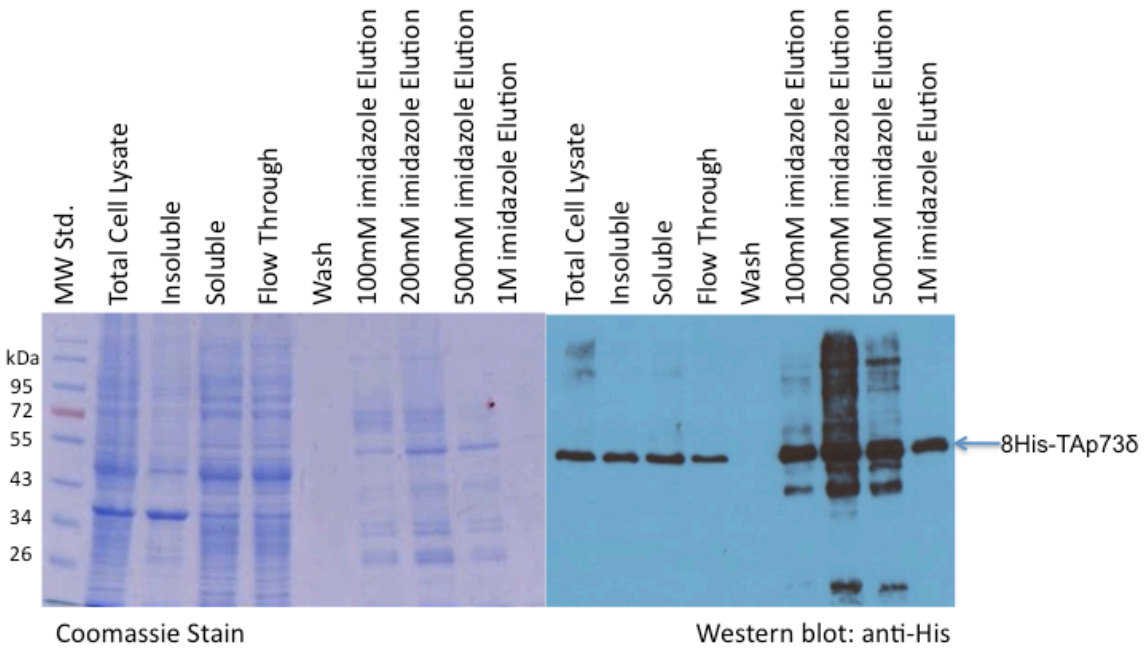

Figure 4.6. Purification of recombinant human 8His-TAp73δ (1-403) using Ni affinity chromatography. Coomassie stain (left) and western blot (right) of 10 % SDS-PAGE analysis showed TAp73α migrated at ~55 kDa.

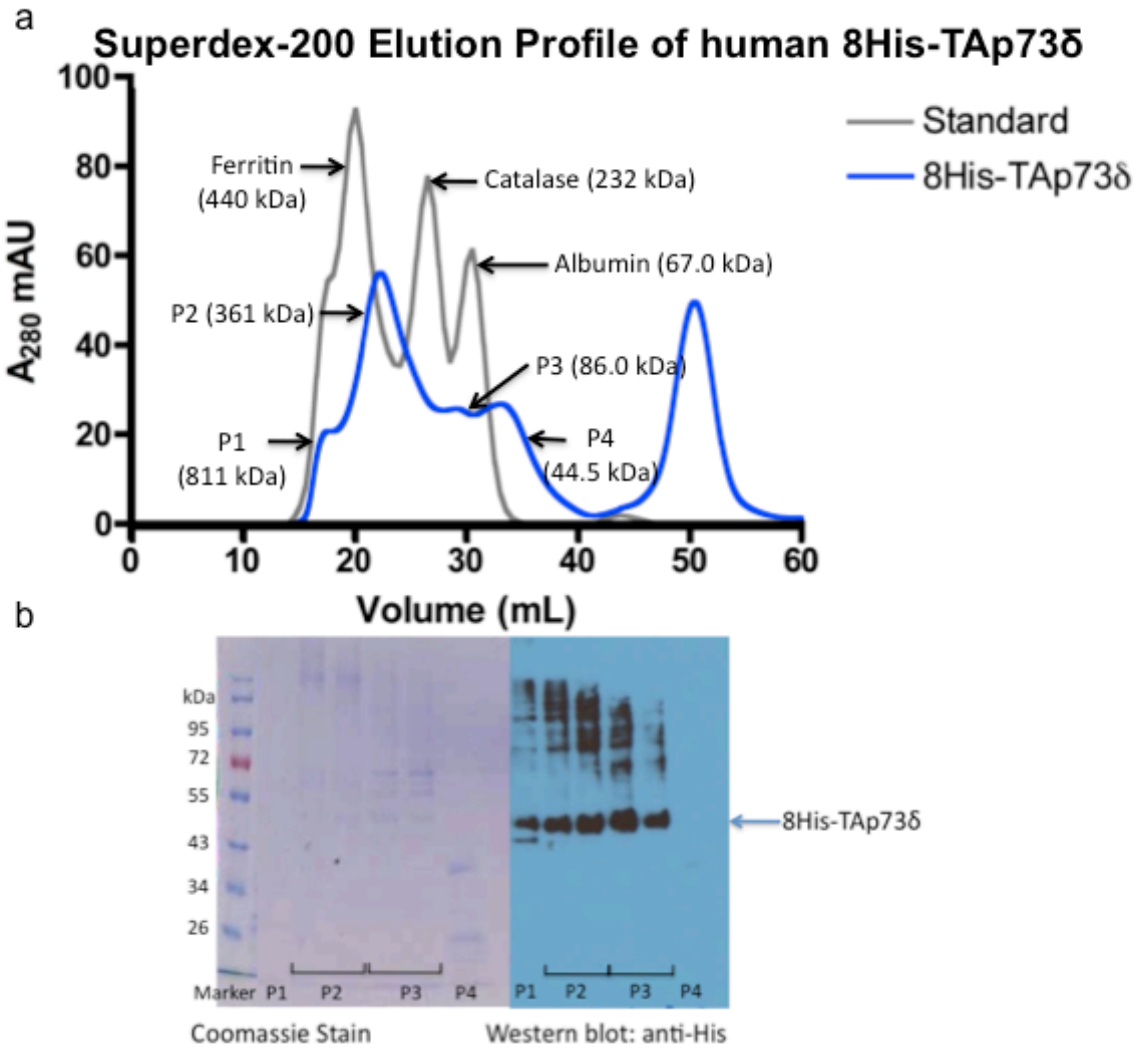

Figure 4.7. Purification of recombinant human 8His-TAp73δ (1-403) using gel filtration chromatography. a) Superdex-200 gel filtration chromatography elution profile. Overlaying with MW standard indicates 8His-TAp73δ eluted as large MW oligomers (P2). b) 10 % SDS-PAGE analysis of superdex-200 elutions.

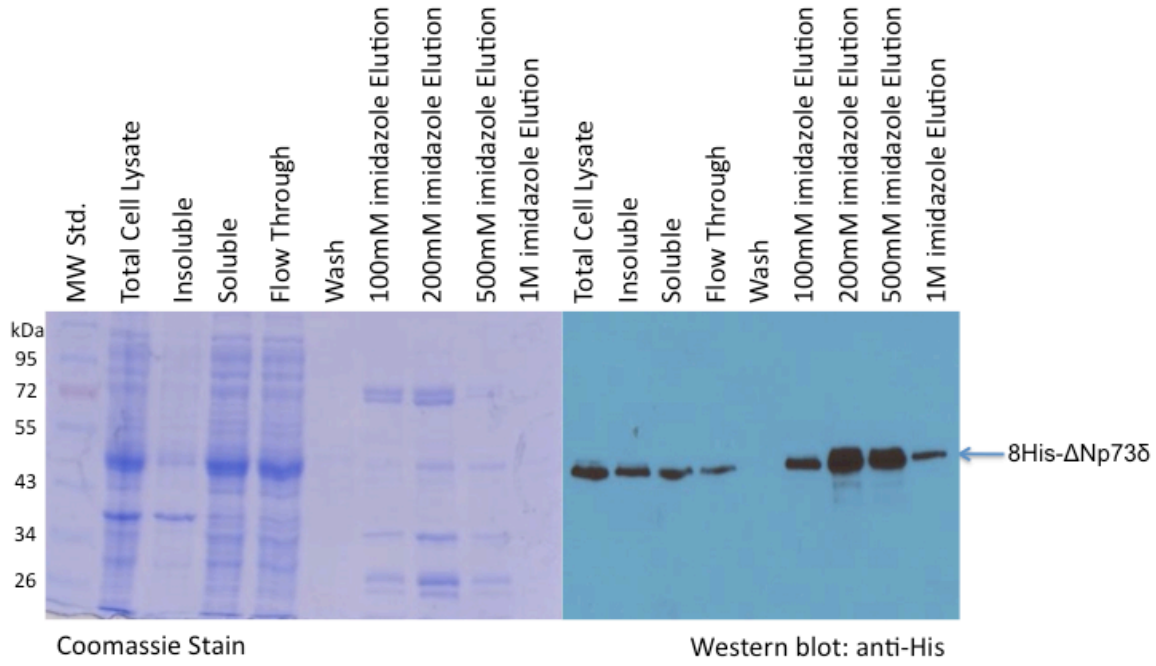

Figure 4.8. Purification of recombinant human 8His-ΔNp73δ (1-354) using Ni affinity chromatography. Coomassie stain (left) and western blot (right) of 10 % SDS-PAGE analysis showed TAp73α migrated at ~50 kDa.

D. Discussion

I have successfully expressed and purified 8His-tagged full-length TAp73α and N-terminal truncated ΔNp73α isoform in *E. coli* using Ni affinity chromatography. These two isoforms assembled into tetramers in solution. However, the yields of these two protein isoforms were not sufficient to carry on other functional studies such as analytical ultracentrifugation or fluorescence anisotropy to determine DNA binding affinity.

Recombinant 8His-TAp73δ isoform was also successfully expressed and purified in *E. coli*. However, it appeared as large MW oligomers (MW is ~361 kDa, which is larger than the expected MW of a tetramer) in gel filtration chromatography. Other techniques such as analytical ultracentrifugation and small-angle light scattering could be employed to further study the protein oligomerization state in solution.

Large amounts of highly pure protein of all these isoforms are required for further functional studies. Currently, our lab is still optimizing the expression and purification system for all the isoforms by employing different affinity tags and alternative chromatography strategies such as ion exchange chromatography. We could also investigate other expression systems in the future such as baculovirus and mammalian systems since certain post-translational modifications such as phosphorylations are lacking in bacteria. Therefore, the protein might not be folded properly and functionally active in bacteria due to the lack of critical post-translational modifications.

E. References

De Laurenzi, V., Costanzo, A., Barcaroli, D., Terrinoni, A., Falco, M., Annicchiarico-Petruzzelli, M., Levrero, M., and Melino, G. (1998). Two new p73 splice variants, gamma and delta, with different transcriptional activity. The Journal of experimental medicine *188*, 1763-1768.

De Laurenzi, V.D., Catani, M.V., Terrinoni, A., Corazzari, M., Melino, G., Costanzo, A., Levrero, M., and Knight, R.A. (1999). Additional complexity in p73: induction by mitogens in lymphoid cells and identification of two new splicing variants epsilon and zeta. Cell death and differentiation *6*, 389-390.

Kaghad, M., Bonnet, H., Yang, A., Creancier, L., Biscan, J.C., Valent, A., Minty, A., Chalon, P., Lelias, J.M., Dumont, X.*, et al.* (1997). Monoallelically expressed gene related to p53 at 1p36, a region frequently deleted in neuroblastoma and other human cancers. Cell *90*, 809-819.

Ueda, Y., Hijikata, M., Takagi, S., Chiba, T., and Shimotohno, K. (2001). Transcriptional activities of p73 splicing variants are regulated by inter-variant association. The Biochemical journal *356*, 859-866.

Yang, A., Walker, N., Bronson, R., Kaghad, M., Oosterwegel, M., Bonnin, J., Vagner, C., Bonnet, H., Dikkes, P., Sharpe, A.*, et al.* (2000). p73-deficient mice have neurological, pheromonal and inflammatory defects but lack spontaneous tumours. Nature *404*, 99-103.